ARL-SR-0474 ● JULY 2023

6th Annual Postdoc and Early Career Research Day: DEVCOM Army Research Laboratory's Poster Symposium and Activities

by Alexander Bassett, Ibrahim Boulares, Sebastin Carrasco, Stephen Cluff, Kathleen Coleman, Catherine Dillier, Benjamin Evangelisti, Dov Fields, Mary Beth Galanko, Felix Gervits, James Hare, Joshua Hill, Robert Jane, Haval Kareem, Mark Kozlowski, LeighAnn Larkin, David McLeod, Vijay Parameshwaran, Glenn Pastel, Jake Perazzone, Italo'Ivo Lima Dias Pinto, Nuttida Rungratsameetaweemana, Je Ir Ryu, Jonah Sengupta, Dinesh Thapa, Garrett Tow, Malgorzata Turalska, Elliot Wainwright, and Jose Wippold

NOTICES

Disclaimers

The findings in this report are not to be construed as an official Department of the Army position unless so designated by other authorized documents.

Citation of manufacturer's or trade names does not constitute an official endorsement or approval of the use thereof.

Destroy this report when it is no longer needed. Do not return it to the originator.

ARL-SR-0474 ● JULY 2023

6th Annual Postdoc and Early Career Research Day: DEVCOM Army Research Laboratory's Poster Symposium and Activities

by Alexander Bassett, Ibrahim Boulares, Stephen Cluff, Kathleen Coleman, Mary Beth Galanko, Felix Gervits, James Hare, Joshua Hill, Robert Jane, Haval Kareem, Mark Kozlowski, LeighAnn Larkin, David McLeod, Vijay Parameshwaran, Glenn Pastel, Jake Perazzone, Jonah Sengupta, Elliot Wainwright, and Jose Wippold
DEVCOM Army Research Laboratory

Sebastin Carrasco, Catherine Dillier, Dov Fields, Italo'Ivo Lima Dias Pinto, Nuttida Rungratsameetaweemana, Je Ir Ryu, Dinesh Thapa, Garrett Tow, and Malgorzata Turalska
Oak Ridge Associated Universities

Benjamin Evangelisti
The Pennsylvania State University

REPORT DOCUMENTATION PAGE

Form Approved
OMB No. 0704-0188

1. REPORT DATE *(DD-MM-YYYY)*	2. REPORT TYPE	3. DATES COVERED (From - To)
July 2023	Special Report	22 September 2021

4. TITLE AND SUBTITLE
6th Annual Postdoc and Early Career Research Day: DEVCOM Army Research Laboratory's Poster Symposium and Activities

5a. CONTRACT NUMBER

5b. GRANT NUMBER

5c. PROGRAM ELEMENT NUMBER

6. AUTHOR(S)
Alexander Bassett, Ibrahim Boulares, Sebastin Carrasco, Stephen Cluff, Kathleen Coleman, Catherine Dillier, Benjamin Evangelisti, Dov Fields, Mary Beth Galanko, Felix Gervits, James Hare, Joshua Hill, Robert Jane, Haval Kareem, Mark Kozlowski, LeighAnn Larkin, David McLeod, Vijay Parameshwaran, Glenn Pastel, Jake Perazzone, Italo'Ivo Lima Dias Pinto, Nuttida Rungratsameetaweemana, Je Ir Ryu, Jonah Sengupta, Dinesh Thapa, Garrett Tow, Malgorzata Turalska, Elliot Wainwright, and Jose Wippold

5d. PROJECT NUMBER

5e. TASK NUMBER

5f. WORK UNIT NUMBER

7. PERFORMING ORGANIZATION NAME(S) AND ADDRESS(ES)
DEVCOM Army Research Laboratory
ATTN: FCDD-RLA-WB
Adelphi, MD 20783-1138

8. PERFORMING ORGANIZATION REPORT NUMBER
ARL-SR-0474

9. SPONSORING/MONITORING AGENCY NAME(S) AND ADDRESS(ES)

10. SPONSOR/MONITOR'S ACRONYM(S)

11. SPONSOR/MONITOR'S REPORT NUMBER(S)

12. DISTRIBUTION/AVAILABILITY STATEMENT
DISTRIBUTION STATEMENT A. Approved for public release: distribution unlimited.

13. SUPPLEMENTARY NOTES

14. ABSTRACT
The DEVCOM Army Research Laboratory (ARL) Postdoctoral Association organized its 6th Annual Postdoc and Early Career Research Day on 22 September 2021 to showcase research outcomes, achievements, and contributions from postdocs and early career researchers across the enterprise. The event included a series of invited speakers, a Q&A panel, and a poster session.
This special report contains a summary outlining the event and a snapshot of ARL's postdoctoral and early career research communities in the Fall of 2021. The abstracts presented at the event and a limited number of contributed posters are appended.

15. SUBJECT TERMS
ARL Postdoc and Early Career Research Day, ARL Postdoc Association, ARL Early Career Working Group, 2021 Postdoc Week, poster symposia

16. SECURITY CLASSIFICATION OF:			17. LIMITATION OF ABSTRACT	18. NUMBER OF PAGES	19a. NAME OF RESPONSIBLE PERSON
a. REPORT	b. ABSTRACT	c. THIS PAGE			LeighAnn Larkin
Unclassified	Unclassified	Unclassified	UU	51	19b. TELEPHONE NUMBER (Include area code) (301) 394-1430

Contents

List of Figures

List of Tables

Acknowledgments

The organizing committee of the 6th Annual Postdoc and Early Career Research Day was composed of the 2020–2021 Postdoctoral Association (PDA) cochairs, Drs Stephen Cluff and LeighAnn Larkin. The PDA would like to acknowledge those who assisted with planning, coordinating, and volunteering at the symposium. First and foremost, the committee would like to acknowledge the invited speakers at our event: Dr Rose Pesce-Rodriguez, SGMT Luke Blum, Ms Sarah Wheat, Ms Cheryl (Renee) Bitner, Dr Michael Wraback, Dr John LaScala, and Dr Greg Lieberman. We would like to acknowledge the judges for the poster and oral component of the symposium: Drs David Baker, Richard Becker, Nicholas Jankowski, Barbara Nichols, Rose Pesce-Rodriguez, Randy Thompkins, Adam Wilson, Chi-Chin Wu, Tess Zu, Jeff Lloyd, and Jeffrey Veals. This year's event was hosted virtually on the ARL Café channel with the assistance of Dr Greg Lieberman and Ms Ashley Eidsmore. The PDA would also like to acknowledge the presenters and attendees of the symposium.

1. Introduction

The DEVCOM Army Research Laboratory's (ARL) Postdoctoral Association (PDA) is an organization that was established by and is composed of ARL postdocs. The PDA was formed with the mission of improving the postdoctoral experience by facilitating an organization-wide culture of inclusive connection amongst the cohort of early researchers. The PDA executes this goal by organizing events aimed at the professional growth of postdocs at ARL. The annual research day is the PDA's flagship event designed to highlight the research performed by our postdocs. This special report contains a summary of the day's events as well as commentary on the event, including laboratory engagement, successful aspects, and future improvements. Abstracts and a limited number of contributed posters are also included in the appendixes.

2. Summary of Events

The 6th Annual Postdoc and Early Career Research Day (6PECRD) was held on September 22, 2021, to coincide with the 2021 National Postdoc Appreciation Week (NPAW). Like NPAW, the goal of 6PECRD was to bring awareness to the important research being performed by postdocs and early career researchers across the organization, promote collaboration where suited, and create a space for postdocs to network within ARL. Most importantly, the 6PECRD provided a venue to celebrate and promote the postdoctoral and early career experience at ARL.

The 6PECRD was held virtually on the ARL Café channel. Historically, the event has been held on-site at either the Aberdeen Proving Ground (APG) or Adelphi Laboratory Center (ALC) location. The COVID-19 pandemic led to the symposium being moved onto a virtual platform for both the 2020 and 2021 symposiums. Best practices and lessons learned, discussed in further detail in Section 3, were incorporated into planning the virtual aspect of 6PECRD. In summary, the presenters were divided into groups of three to four, based on their directorate. Each group of researchers was given their own virtual meeting room where two to three judges, also from the shared directorate, were assigned. This approach ensured that each presenter had an audience of at least five researchers from their own directorate. Each presenter was given 15 min to present their poster and answer questions. An assigned judge in each room ensured minimal deviation from the schedule and reduced tangential discussions.

In addition to the research portion of the 6PECRD, the PDA organized two additional featured presentations. The first, titled "Programs YOU should know about at ARL!" included three 15-min "flash presentations" presented by the

following personnel, to promote awareness of ongoing networking and professional development opportunities at ARL.

- Ms Cheryl (Renee) Bitner – "Resources and programs available through the ARL Civilian Human Resources Office (CHRO)"
- Sergeant Major (SGM) Luke Blum: "ARL Civilian Greening Course"
- Ms Sarah Wheat – "ARL Mentoring Program"

The second presentation, "Success at ARL," featured three successful ARL scientists: Drs Michael Wraback, John LaScala, and Gregory Liebermann, who each discussed their career trajectories at ARL and gave advice to the early career cohort about how to make the most of their time at ARL. Further discussion on the featured presentations can be found in Section 4 and 5.

3. Engagement across the Laboratory

A total of 26 postdocs and early career researchers presented their research at the symposium. The names and affiliated organization of the presenters can be found in Table 1. Select abstracts and posters are found in Appendixes A and B, respectively.

Data on the number of postdocs and their affiliated directorates has been maintained for the past four symposiums and is given in Figure 1. The 2021 symposium saw a drop in the number of presenters from previous years. The event was primarily advertised through the ARL Dispatch and ARL Café and did not benefit from the "word of mouth" advertisement that took place prior to the move to remote work during the pandemic. Additionally, the number of postdoctoral researchers at ARL has decreased in recent years.

While the number of presenters was lower than in past years, the event was well attended by the workforce. For most sessions, there were typically 15–20 participants (including the judges and presenters). At the featured flash presentations, outlined in Section 1, attendance fluctuated between 64 and 74 participants. At the "Success at ARL" Q&A featured event, attendance fluctuated between 58 and 60 participants. The PDA believes the high attendance at the featured presentations was since the programs were held virtually and were therefore widely accessible.

Table 1 List of postdoctoral fellows who presented at the 2021 symposium

Presenter	Directorate	Location
Bassett, Alexander	WMRD	APG
Boulares, Ibrahim	SEDD	ALC
Carrasco, Sebastin	CISD	ALC
Cluff, Stephen	WMRD	APG
Coleman, Kathleen	SEDD	ALC
Evangelisti, Benjamin	WMRD	APG
Fields, Dov	CISD	ALC
Galanko, Mary Beth	SEDD	ALC
Gervits, Felix	CISD	ARL-NE
Hare, James	CISD	ALC
Hill, Joshua	SEDD	ALC
Jane, Robert	SEDD	ALC
Kareem, Haval	SEDD	ALC
Kozlowski, Mark	WMRD	APG
Mcleod, David	WMRD	APG
Parameshwaran, Vijay	SEDD	ALC
Pastel, Glenn	SEDD	ALC
Perazzone, Jake	CISD	ALC
Pinto, Italo′Ivo Lima Dias	HRED	APG
Rungratsameetaweemana, Nuttida	HRED	APG
Ryu, Je Ir	CISD	APG
Sengupta, Jonah	WMRD	APG
Thapa, Dinesh	WMRD	APG
Tow, Garrett	WMRD	APG
Turalska, Malgorzata	CISD	ALC
Wainwright, Elliot	WMRD	APG
Wippold, Jose	HRED	ALC

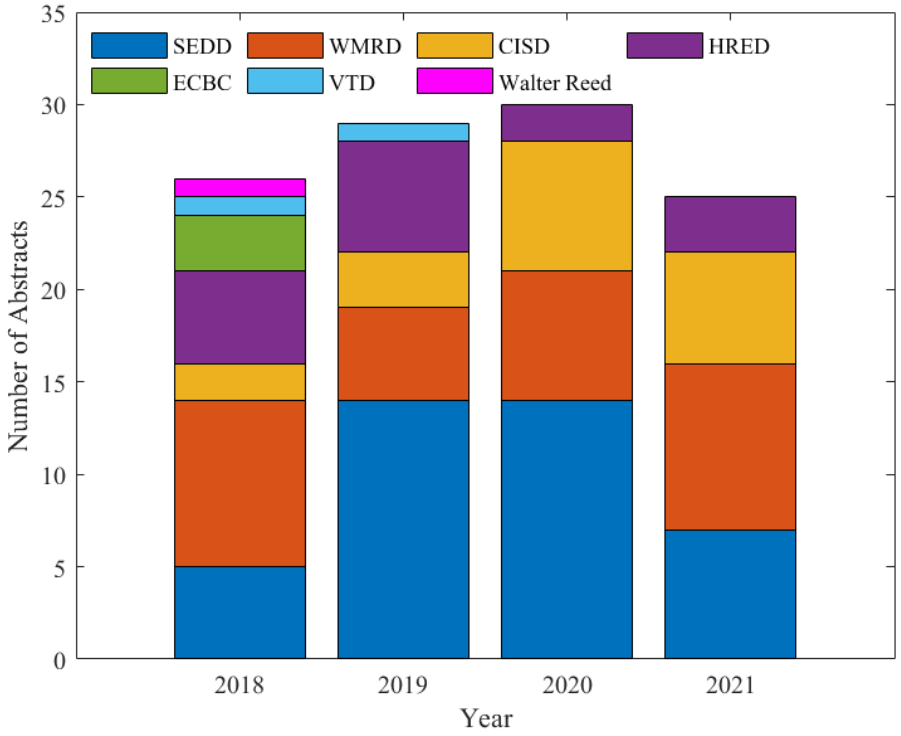

Fig. 1 Number of abstracts submitted to the postdoc research symposium over the past 4 years (representation from the various directorates is shown). The VTD directorate was dissolved in 2020.

4. Hosting the Research Symposium Virtually: PDA Perspective

The 2020 conference was the first to be hosted virtually on the ARL Café. After action discussions were held with a select group of the presenters and judges to identify best practices to enhance the overall experience of the presenters, especially regarding the virtual aspect of the event. During the 2020 conference, each presenter was placed in their own room where the judges and visitors could stop by. The most valuable feedback provided by presenters was that their rooms were not given enough "virtual foot traffic." Thus, the PDA elected to organize virtual "rooms" of posters that would host three to four presenters. This ensured that at least three of their peers and two to three judges, would view their presentation. Since participants were organized into rooms based on their directorate, participants in each room would likely have a common background knowledge of the topics being presented. Feedback received after the 2021 event demonstrated a positive trend in the presenters' feelings about their perceived audience and reach. The downside to this format was that it did not facilitate a significant amount of cross-directorate discussion and that it was not as conducive to the poster-style presentation (i.e., all content on a single slide). Going forward,

the PDA has decided to transition from poster-based to short, multi-slide presentations.

The 6PECD was also the first conference hosted completely within the ARL Café (Technical Events channel). As a result, the event was automatically added to the calendar of any ARL staff member who subscribed to ARL Café, clicking on the calendar event lead directly to the rooms with the day's events. We believe this led to significant workforce participation throughout the day. We aim to host all future virtual PDA-sponsored events on the ARL Café. Additionally, the conference itinerary, presentations, and abstracts are all permanently available to anyone with ARL Café access under the Technical Events Wiki page.

5. Lessons Learned from 6PECRD

The PDA board would like to conclude this special report with a summary of lessons learned and best practices for future research symposia. Key practices adopted include:

- Hosting the symposium on days that allowed for the greatest participation of invited guests (Tuesday, Wednesday, or Thursday).
- Hosting the event on the ARL Café channel made the event widely accessible to the entire workforce.
- Having a full itinerary (complete with hyperlinks to all the virtual rooms/events) on the ARL Café channel enabled wide participation by the workforce.
- Advertising in several special dispatches to the full ARL workforce is an effective way to publicize the event. At a minimum, one Special Dispatch announcing the symposium and one very close to the day of the event complete with hyperlinks to each room.

There were some notable themes and topics that were brought up several times within the Q&A session and the flash presentation that the PDA feels are worth mentioning for future planning committees. Early career staff are interested in better understanding:

- How individual projects fit into larger mission research programs.
- How the research conducted at ARL helps the warfighter.

Appendix A. Contributed Abstracts Presented at the 6th Postdoc and Early Career Research Day*

* The contents of this appendix appear in original form, without editorial change.

Design of Experiments to Detonative Performance: Energetic, Acrylate-Nitramine Polymer Formulations for Polymer-Bonded Explosives

Bassett, Alexander W.[1], Munson, C. A.[1], Reid, T. A.[1], Clay, A. M.[2], and Banning, J. E.[1]*

[1]CCDC Army Research Laboratory, **FCDD-RLW-WB**, APG, MD, [2]CCDC Army Research Laboratory, **FCDD-RLW-MD**, APG, MD

*corresponding author: alexander.w.bassett2.civ@army.mil

Binders used in polymer-bonded explosive (PBX) formulations provide a matrix for the encapsulation of high energy (HE) solid fills. Conventional PBX binders are inert materials that decrease the energetic performance of the bulk PBX, therefore the replacement of conventional binders with energetic substitutes provides a strategy for improving the total PBX detonative performance; however, efforts must be made to ensure that the binder properties are not sacrificed to achieve such gains. In an effort to produce binder formulations with desired thermal and mechanical performance with increased detonative properties, nitramine based building blocks were identified and formulated via a Design of Experiments (DOE) approach to explore the relationships between the relative composition of individual binder ingredients and HE fill. Structure-property relationships of the acrylate-nitramine binder demonstrated that increasing molecular weight between crosslinks (M_c) resulted in lower values of glass transition temperature (T_g), as well as the ability to load higher amounts of plasticizer within the polymer matrix. Based on these results, an optimized formulation can be achieved whereby T_gs can range from – 27 °C to – 7 °C without significant impact to predicted detonative performance. In many cases the formulation can be tailored to exceed the predicted detonative performance of PBXN-110.

Infrared Optical-Field-Driven Luminescence in Quantum Dots

Boulares, Ibrahim[1], Connelly, B. C.[1], Gao, F. Y.[2], Shi, J.[2], Zhang, Z.[2], and Nelson, K. A.[2]*

[1]CCDC Army Research Laboratory, **FCDD-RLS-ED**, Adelphi, MD, [2]Department of Chemistry, Massachusetts Institute of Technology, Cambridge, MA

*corresponding author: ibrahim.boulares.civ@army.mil

In a recent study on CdSe-CdS core-shell colloidal quantum dots (QDs) it was shown that extreme electric fields from ultrafast THz-frequency electromagnetic pulses alone can produce QD luminescence [1, 2]. Unlike in the multi-photon absorption process, which occurs at much higher optical frequencies, such emission was shown to be associated with large energy shifts of the absorption edge (more than 25%) – much like electro-luminescence (EL) driven by a quasi-DC field. While details of the mechanism of THz driven-EL are still under investigation, the effects of high optical electric fields of mid- to long- wavelength infrared radiation on the optical properties of QDs remain largely unexplored. To expand our understanding of the responses of QDs to extreme optical fields, we investigated the interaction of various visible bandgap QD materials with sub-picosecond infrared-frequency pulses in the 3.5 to 12 micron wavelength range, at electric field levels that exceeded 1 MV/cm. We observed significant luminescence, resulting in up-conversion of the infrared light to visible wavelengths, throughout the mid-IR range that we explored. Additional results from investigations of the photoluminescence lifetime dependence on the sub-bandgap excitation wavelength and power of the excitation beam suggests similar electroluminescence induced by strong THz and IR fields.

[1] Brandt C. Pein et al., Nano Lett. 17, 5375 (2017).

[2] https://doi.org/10.1021/acs.nanolett.9b03342.

Towards the optimal squeezed states: an optimal control approach

Carrasco, Sebastián[1], Goerz, M.[1], Vuletić, V.[2], and Malinovsky, V.S.[1]*

[1]CCDC Army Research Laboratory, **FCDD-RLC-NT**, Adelphi, MD, [2]Department of Chemistry, Massachusetts Institute of Technology, Cambridge, MA

*corresponding author: seba.carrasco.m@gmail.com

In recent decades atom interferometry has evolved into a versatile tool with unmatched precision, leading to unprecedented achievements in the demonstration of quantum phenomena, measurement of fundamental constants, and inertial sensing. Recently, it has been demonstrated that the usage of correlated states, such as spin squeezed states, can boost the precision of this apparatus by orders of magnitude, *i.e.*, going beyond what is known as the standard quantum limit. These states could provide a new generation of gravity gradiometers to achieve sensitivities of several orders of magnitude higher than conventional ones, allowing them to detect dense materials in sub-surface structures, which is of immediate interest to the Army. Similarly, atomic clocks based on the same principles will enhance geodesic measurements, communication, and navigation.

One notable experimental realization of spin squeezing is carried on by the group of Prof. Vuletic at MIT in the form of an optical lattice clock. In this device, the preparation of these non-trivial states relies on precise manipulation in the form of laser pulses to create a specific kind of effective interaction between atoms called one-axis twisting, which also compromises the capability of reaching the optimal squeezed state. Our results show that by applying Optimal Control Theory, one can go beyond this limitation while using the effective interaction and standard pulses in a non-trivial way, *i.e.*, increasing sensitivity while using the current experimental capabilities. These novel schemes should also be applicable in a similar form to other similar experimental setups.

The Effect of Varying Laser Power on the Prior Austenite Structure of DED Processed AF9628 Steel

Cluff, Stephen [1], Mock, C.[1], and Sinha, V.[2]*

[1]CCDC Army Research Laboratory, **FCDD-RLW-MD**, APG, MD, [2]UES Inc., Dayton, OH

*corresponding author: stephen.r.cluff2.civ@army.mil

The computational reconstruction of the prior austenite phase in martensitic steels allows for the observation of the effect of manufacturing parameters on intermediate microstructures during processing. This information is valuable both for the characterization of the material generally, as well as in the effort to model the effects of changing processing parameters on final material microstructure. In this work, thin walls of AF9628 steel are formed using the directed energy deposition (DED) additive method and observed via electron back-scatter diffraction (EBSD) imaging. The prior austenite grains are computationally reconstructed in MATLAB to observe the morphology of the austenite grains in samples that were formed using different laser powers. The size and the shape of the parent austenite grains are compared and contrasted. Future work will build on this characterization of AF9628 to build models of microstructure formation in AF9628 during the DED process.

Flexible Low SWaP-c Electric and Magnetic Field Sensors

Coleman, Kathleen [1], Heintzelman, S.[1], Tsang, H.[1], and Hull, D.[1]*

[1]CCDC Army Research Laboratory, **FCDD-RLS-EM**, ALC, MD,

*corresponding author: kathleen.p.coleman2.ctr@army.mil

With the increasing need for always-on and long-lasting sensing, electric- and magnetic-field sensors are designed to cover vast ranges without interruption. Current sensors have high sensitivity, cover large ranges, are costly, and require high power (0.1-10 W). As a result, these sensor systems tend to be bulky, as they require large energy storage units. Many times these sensors are heavily

duty cycled to increase their lifespan, and therefore they miss large amounts of data. Additionally, this sensing method is extremely vulnerable, since it depends on one sensor for the wide range. This work explores a more resilient sensing paradigm, where a series of low size weight power and cost (SWaP-c) sensors cover the same range, reducing the reliance on an individual sensor node. This work outlines the technical areas, including low-power electronics, novel energy harvesting and storage capabilities, and flexible electronics, required for creating low SWaP-c sensor nodes. Initial work explores ways to reduce the average power of the sensor system to ~1 mW in order to be small and compatible with novel energy harvesting methods, which have power densities of 0.1-10 mW/cm^2. To make smaller conformal sensors, the sensor's printed circuit board is printed using flexible electronics, and the electrical and mechanical robustness of the Cu-flex board is being evaluated. By incorporating these technologies, low SWaP-c sensors can be readily used for more robust and advanced sensing networks.

Understanding Small Molecule Interactions on Alumina Surfaces Using Reactive Molecular Dynamics Simulations

Evangelisti, Benjamin [1], Wu, C.[2], Thapa, D.[2], and Anstine, D. M.[3]*

[1]Chemistry Department, The Pennsylvania State University, State College, PA, [2]CCDC Army Research Laboratory, **FCDD-RLW-WA**, APG, MD, [3]Department of Materials Science and Engineering, University of Florida, Gainesville, FL

*corresponding author: benjamin.evangelisti@gmail.com, bue33@psu.edu

Aluminum nanoparticles (n-Al) have been the subject of significant study with a focus on modifying and functionalizing the inactive alumina shell (amorphous Al_2O_3). The oxide shell occupies a significant portion of the particle leading to a decreased active energy content for combustion and reduced energy release rates. At the US Army Combat Capabilities Development Command Army Research Laboratory (DEVCOM ARL), carbonaceous-coated energetic n-Al have been successfully produced from commercial n-Al via carbon monoxide (CO) /helium (He) plasma treatment which produces an alumina surface that is functionalized with aluminum carboxylates and hydroxyl groups. This work used reactive molecular dynamics simulations using a publicly available ReaxFF potential to study the effects of amorphous (a-Al_2O_3) and α-phase alumina (α-Al_2O_3) surfaces on the sorption and dehydrogenation of small molecules including water, methane, and formic acid. The dehydrogenation barrier for water on the a-Al_2O_3 surface was found to be lower than its corresponding desorption barrier while the dehydrogenation barrier for water on the α-Al_2O_3 surface was found to be greater than its corresponding desorption barrier suggesting that most water dehydrogenation occurs away from the surface. This dehydrogenation barrier was observed to decrease on the a-Al_2O_3 with the addition of another surface water molecule nearby. The dehydrogenation barrier for formic acid was slightly lower than its corresponding desorption barrier on a-Al_2O_3. However, this was not observed on the α-Al_2O_3 surface. The methane dehydrogenation barrier was also lower than its corresponding desorption barrier suggesting that aliphatic carbons may participate in alumina hydroxyl formation. Overall, this work advances understanding on different alumina surfaces interacting with representative small molecules relevant to experiments.

A Generalized Approach to Two Qubit Linear-Optical State Analyzers

Fields, Dov [1], Bergou, J.[2], Hillery, M.[2], and Malinovsky, V. S.[1]*

[1]CCDC Army Research Laboratory, **FCDD-RLC-NT**, Adelphi, MD, [2]Department of Physics and Astronomy, Hunter College, New York, NY

*corresponding author: dovfields@gmail.com

Linear optical technology is a critical to the construction and implementation of quantum networks. A key requirement of any such system is the successful measurement of quantum states. This poses a particular challenge for linear optical systems, which are severely limited in their ability to discriminate between orthogonal entangled states. For instance, the maximally entangled Bell States can only be discriminated with a 50% success probability, when no ancillary photons are allowed. The optimal protocol is known for Bell States, but not for more general orthogonal states. The goal

of our work is to give a general approach for constructing optimal discrimination protocols for any arbitrary set of orthogonal two-qubit optical states for linear optical setups with no ancillary photons. These results will hopefully lead to improving the potential result of linear optical protocols for systems where non-maximally entangled states are present.

Frequency Scaling of Passive Voltage Gain in 1-port Quartz Resonators

Galanko, Mary Beth [1], Bedair, S. S.[1], Keibala, T. B..[1], Diamond, D.[2], Rudy, R.[3], and Tseng, V. F-G.[1]*

[1]CCDC Army Research Laboratory, **FCDD-RLS-CC**, Adelphi, MD, [2]Department of Electrical and Microelectronic Engineering, Rochester Institute of Technology, Rochester, NY, [3]CCDC Army Research Laboratory, **FCDD-RLS-SA**, Adelphi, MD

*corresponding author: mary.e.galanko.civ@army.mil

This work investigates 1-port thickness-shear mode quartz resonators for filtering and voltage gain in a radio frequency (RF) wake-up receiver (WUR). A WUR consumes "near-zero" power (<< 100 nW) while monitoring for an RF signal of interest, and upon detection of this signal, activates other hardware with additional capabilities and higher power consumption. This approach ensures minimum power consumption and maximum battery life for the system as a whole. Applications range from consumer "Internet of Things" (IoT) to Army environment monitoring. Achieving high sensitivity at very low false-alarm rate and power consumption remains a challenge in WUR design. The piezoelectric devices in this work simultaneously offer passive voltage gain, impedance matching, and high quality factor (Q_m) resonant filtering in the WUR front-end. Until recently, RF voltage gain had been demonstrated in these devices only at frequencies ≤ 76 MHz. To assess performance over a broad frequency range, this work examines devices with varying frequency (50-200 MHz), geometry, and capacitance. Active probes present various load impedances while precisely measuring voltage gain and Q_m. Overall, measurements of loaded gain, Q_m, and figure of merit (FoM = $Q_m \times k^2$) validate model predictions. Furthermore, devices around 200 MHz demonstrate higher Q_m than previously predicted. Voltage gain 220 V/V is demonstrated at $f_r \approx 184.5$ MHz, the highest gain directly measured in a piezoelectric microresonator around this frequency. Subject to post-fabrication variation, these results are repeatable in a commercial quartz process, enabling widespread use of this technology.

Learning through Dialogue for Soldier-Robot Interaction

Gervits, Felix

[1]ARL-Northeast, FCDD-RLC-IT, Burlington, MA

*corresponding author: felix.gervits.civ@mail.mil

Robots working alongside humans in novel environments will readily come across objects, actions, and tasks that they do not know about. As a result, mechanisms are needed for the robots to learn about these novel concepts through dialogue with humans. This is critical for future Army missions which will have artificial agents (e.g., Next Generation Combat Vehicle) embedded in human teams making decisions in the physical world. To achieve the goal of learning through dialogue, we first ran an empirical study to investigate how people ask questions in novel environments. The labeled dialogue and video data from the study were curated and released as the HuRDL (Human Robot Dialogue Learning) Corpus. Based on this corpus, we created a computational model for automated question generation using a decision-theoretic approach. The model uses a decision network, which is a graphical probabilistic model that allows a robot to represent uncertainty across multiple modalities, to ask clarification questions that maximize expected utility, and to learn from the responses. The model is generalizable in that it can be

used in a variety of different environments without the need for extensive training data. We have integrated the model into the DIARC (Distributed Integrated Affect Reflection Cognition) robotic architecture from our collaborators at Tufts University and developed a proof-of-concept

demonstration showing a robot learning about novel concepts through dialogue with a human. The demonstration shows that this approach is feasible for achieving our research goals, and can be transitioned in the future for Army applications.

Toward Uncertainty Aware Quickest Change Detection

Hare, James Z. [1] and Kaplan, L.[1]*

[1]CCDC Army Research Laboratory, **FCDD-RLC-CA**, Adelphi, MD

*corresponding author: james.z.hare.civ@army.mil

This work studies the problem of Quickest Change Detection (QCD) where at some unknown deterministic time, observations drawn from the environment change from a pre-change distribution to a post-change distribution and the goal is to develop a test statistic that identifies the change point as quickly as possible. We generalize this problem to conditions where the parameters of both the pre- and post-change distributions are either completely unknown or known within a second-order distribution generated from training data. We propose the use of the Uncertain Likelihood Ratio (ULR) test statistic, which is designed from a Bayesian perspective in contrast with the traditional frequentist approach, i.e., the Generalized Likelihood Ratio (GLR) test, studied in the literature. The ULR test utilizes a ratio of posterior predictive distributions each computed over different segments of the observations. This identifies the expected value of the likelihoods conditioned on the prior and training data collected rather than the likelihoods evaluated with the Maximum Likelihood Estimate (MLE) of the parameters. This approach incorporates parameter uncertainty into the likelihood estimates that naturally arise when there is lack of or limited availability of training samples. Through an empirical study, we show that the proposed test outperforms the GLR test, while achieving similar results as the optimal CUSUM algorithm as the number of training samples goes to infinity. Furthermore, we qualitatively explain the advantages of the ULR over the GLR by comparing their mathematical forms.

Incoherent Dark State Repumping of Rb Rydberg Atoms for Electric Field Sensing

Hill, Joshua C. [1] and Meyer, D. H.[1]*

[1]CCDC Army Research Laboratory, **FCDD-RLS-SQ**, Adelphi, MD

*corresponding author: joshua.c.hill49.civ@army.mil

Rydberg states of alkali atoms, where the valence electron is excited to a high principle quantum number, offer multiple applications of interest to the Army. For example, the large electric polarizabilities of Rydberg states make them an attractive platform for communication receivers via electric field sensing. Energy shifts in the atomic spectra are inherently sensitive to a wide range of incident frequencies, and can be probed using standard optical and RF spectroscopic techniques. Room temperature vapor cells of such atoms can be implemented in a small volume. We probe Rb atoms in Rydberg states using a two-photon electromagnetically induced transparency (EIT) scheme. In this implementation, a portion of the excited atoms decay to an optically dark hyperfine ground state where they no longer participate in the probing-excitation cycle during relevant timescales, reducing the signal of merit. This poster presents preliminary data demonstrating optical repumping of atoms out of the dark state via the ^{85}Rb D1 transition ($\lambda \sim 795$nm). We explore a variety of parameter sets, and show that the most advantageous increases the EIT signal by 32%. This repumping scheme's comparatively lost cost and ease of implementation make it a compelling addition to Rb Rydberg EIT experiments at ARL and elsewhere.

Energy and Exergy Based Optimization and Control for Battlefield Energy Awareness

Jane, Robert S. [1], Corey, J.[2], Glass, E.[2], Mossman, E.[2], and Kim, T.[2]*

[1]CCDC Army Research Laboratory, **FCDD-RLS-CP**, Adelphi, MD, [2]Department of Chemistry and Life Science, United States Military Academy, West Point, NY

*corresponding author: robert.s.jane2.civ@army.mil

The outcome of any current or future military engagement will be decided by our ability to transition between efficient and effective use of energy and power. Energy and power management will impact all modalities of military warfare, and by understanding the dissimilar energy flows and their interactions as a function of time, space and the environment we can begin to develop energy awareness. Energy awareness gives rise to a holistic understanding of energy and power consumption, generation, storage, and distribution as a function of mission effectiveness, efficiency, and the operational environment. Using multiple sets of shallow artificial neural networks (SANNs) in combination with deep long short-term memory networks (DLSTMs) we were able to develop a set of computationally efficient predictive algorithms which loosely approximated the energy and exergy flow characterizations of a representative Army platform. The algorithms were combined with a model predictive control (MPC) which permitted the platform to be controlled more optimally in regards to the mission effectiveness in the presence of a silent watch mission. These types of algorithms are paramount in fulfilling the Army's modernization priorities, and will empower profitable operations, well-timed resupply logistics, with improved survivability and lethality. Emerging methods in automated reasoning, such as artificial intelligence, machine learning, etc., represent new, untapped opportunities capable of optimizing energy and power sources and provide transformational change.

Role of Nanophase and Surface Structures of Ternary Nanoalloy Catalysts in Propane Oxidation: A Combined *Operando* Synchrotron X-Ray Diffraction and Diffuse Reflectance Infrared Fourier Transform Spectroscopy Study

Kareem, Haval [1], Langrock A.[1],Leff, A.[1], Auletta, J.[1], Mackie, D.[1], and Tran, D. T.[1]*

[1]CCDC Army Research Laboratory, **FCDD-RLS-CC**, Adelphi, MD

*corresponding author: haval.r.kareem.civ@army.mil

The ability to harness the catalytic oxidation of hydrocarbons is critical for both clean energy production and air pollutant elimination, which requires detailed understanding of the dynamic role of nanophase structure and surface reactivity under the reaction conditions. We report here findings of an in-situ/operando study of such dynamic details of a ternary nanoalloy catalyst under propane oxidation conditions using high-energy synchrotron X-ray diffraction coupled to atomic pair distribution function analysis and diffuse reflectance infrared Fourier transform spectroscopy. The catalysts are derived by alloying Pt with different combinations of second (Pd) and third (Ni) transition metals, showing a strong dependence of the catalytic activity on the Ni content. The formation of different surface intermediates during oxidation of propane is dominated by the favorability to less oxygenation of carbon upon the first C-C bond cleavage followed by more oxygenation of carbon upon the second C-C bond cleavage on the higher-Ni-content ternary catalyst. The dynamic change in the nanophase structure as a result of the formation of surface/subsurface oxygenated metal sites is shown to play an important role in activating and cleaving the O-O and C-C bonds. This finding shines a fresh light on the correlation between the dynamic change of atomic strains and the surface reactivity, a quantitative understanding of which has significant implications for the design of oxidation catalysts with enhanced catalytic activities.

Surface-Display Techniques to Explore Interfacial Interactions of Non-Polar Substrates

Kozlowski, Mark T.[1], Orlicki, J. A.[1], and Pullen, R. M.[2]*

[1]CCDC Army Research Laboratory, **FCDD-RLW-MG**, APG, MD, [2] CCDC Army Research Laboratory, **FCDD-RLH-BA**, Adelphi, MD

*corresponding author: mark.t.kozlowski4.civ@army.mil

Highly non-polar polymers such as polystyrene and polyethylene are very common in the modern world, but their inert characteristics can lead to difficulty forming adhesive bonds. Current approaches to promote adhesion to PS and PE rely on enhancing chain mobility, through the application of elevated temperatures, solvent plasticization, or other pre-treatment. Identifying new strategies to enable good adhesive bonding would provide opportunities for new capacitors, facile repair in the field, and the creation of new composite materials.

In the present work, we explore a class of natural surfactants known as hydrophobins, which are used by fungi to breach air-water interfaces when colonizing new environments[1], and to promote adhesion of the fungi to hydrophobic surfaces.[2] Hydrophobins, and engineered hydrophobin fusion proteins, have already been shown to adhere to highly non-polar surfaces, such as Teflon[3] and polystyrene.[4] Here we display hydrophobins on an E. coli surface using the well-established autotransporter system,[5] and demonstrate adhesion of these bacterial cells using a spot assay, employing substrates such as high-density polyethylene and polystyrene. The on-cell screening is simple, and allows easy genetic manipulation of the hydrophobin. We believe this work will encourage further exploration of biologically-inspired screening methods to explore biotic/abiotic interactions across a wide range of substrates, provide a target for protein engineering, and generate new insights for the exploration of adhesive interfaces.

1. Cox, P. W. & Hooley, P. Hydrophobins: New prospects for biotechnology. *Fungal Biology Reviews* **23**, 40-47, doi:https://doi.org/10.1016/j.fbr.2009.09.001 (2009).
2. Khalesi, M., Gebruers, K. & Derdelinckx, G. Recent Advances in Fungal Hydrophobin Towards Using in Industry. *The Protein Journal* **34**, 243-255, doi:10.1007/s10930-015-9621-2 (2015).
3. Linder, M., Szilvay, G. R., Nakari-Setälä, T., Söderlund, H. & Penttilä, M. Surface adhesion of fusion proteins containing the hydrophobins HFBI and HFBII from Trichoderma reesei. *Protein Sci* **11**, 2257-2266, doi:10.1110/ps.0207902 (2002).
4. Sorrentino, I. *et al.* Development of anti-bacterial surfaces using a hydrophobin chimeric protein. *International Journal of Biological Macromolecules* **164**, 2293-2300, doi:https://doi.org/10.1016/j.ijbiomac.2020.07.301 (2020).
5. Maurer, J., Jose, J. & Meyer, T. F. Autodisplay: One-component system for efficient surface display and release of soluble recombinant proteins from Escherichia coli. *J. Bacteriol.* **179**, 794-804 (1997).

Production of Highly-Crystalline, Free-Standing, Imine-Based 2D Polymer Films

McLeod, David C.[1],Barnes, M. G.[1], and Lambeth, R. H.[2]*

[1]CCDC Army Research Laboratory, **FCDD-RLW-MA**, APG, MD, [2] CCDC Army Research Laboratory, **FCDD-RLW-S**, APG, MD

*corresponding author: david.c.mcleod2.civ@army.mil

Films made from two-dimensional organic polymers are promising materials for a variety of applications, such as membranes for chemical separation, as mechanically-robust engineering materials, and as components of energy storage devices. However, current techniques for synthesizing imine-based 2D polymer films either use methods that are difficult to scale, produce films of only nm-scale thickness, or yield films with modest surface areas and low crystallinity.

Here, a facile, scalable process for casting free-standing, imine-based COF films tens of microns in thickness directly from a solution of monomers in trifluoroacetic acid and water is reported. Highly-crystalline films with surface areas (2,200–2,400 m^2/g) approaching the theoretical maximum could be achieved by controlling the initial film formation conditions and by heating the produced films in ethanol with a small amount of residual acid.

Engineering III-Nitride Semiconductor Materials for Solar-Driven Chemical Energy

Parameshwaran, Vijay[1*]

[1]CCDC Army Research Laboratory, **FCDD-RLS-CC**, Adelphi, MD

*corresponding author: vijay.s.parameshwaran.civ@army.mil

The III-Nitride family of semiconductors (GaN, InN, AlN) and their corresponding ternary alloys ($Al_xGa_{1-x}N$ and $In_xGa_{1-x}N$) forms a basis as a light absorber for solar energy conversion. This research will give an overview of how materials engineering of III-Nitrides is used to design photoelectrode structures that enable conversion of sunlight into hydrogen, syngas, and higher-order hydrocarbon fuels such as ethanol. First, drift-diffusion-Poisson modeling of the energetics at the semiconductor-electrolyte interface shows that controlling the polarization field within single-crystal GaN is critically important for tuning the energetics to run oxidation and reduction reactions. This polarization control is then used to design a photocathode that uses the kinetic energy of accelerated electrons to mitigate catalytic overpotential losses. Second, a growth campaign of III-Nitride epitaxial films and nanowires on (111)-oriented silicon explores the material space of having heterojunctions as electrodes for solar-driven chemical processes, with both GaN and InN showing promise for experiments to elucidate carrier processes at the semiconductor-electrolyte interface. Finally, integration of a copper source within a molecular beam epitaxy system provides a pathway to integrate an effective catalyst for CO_2 reduction processes on a III-Nitride light absorber with a preserved heterointerface and a testbed for experiments to investigate the catalytic behavior of copper-based compounds.

Determining the Active Species in Aqueous Aluminum Electrolyte

Pastel, Glenn[1*], *Schroeder, M.*[1], *Ding, M.*[1], *Pollard, T.*[1], *Ma, L.*[1], *Ho, J.*[1], *Borodin, O.*[1], *and Xu, K.*[1]

[1]CCDC Army Research Laboratory, **FCDD-RLS-LE**, Adelphi, MD

*corresponding author: glenn.r.pastel.civ@army.mil

Recent reports on aqueous aluminum electrolyte boast impressive metrics including low cost, high energy density, and robust safety, however the solvation environment and ion transport of trivalent aluminum is not well understood, particularly in the high concentration regime. This study provides compelling evidence for high activity of hydronium (H_3O^+) rather than aluminum (Al^{3+}) in aqueous Al trifluoromethanesulfonate (Al triflate, $(CF_3SO_3)_3Al$) electrolyte. These findings are rooted in the solvation structure of the aluminum ions as revealed by spectroscopic analysis, as well as the electrochemical stability of the electrolyte components. Additional concerns regarding the solvation environment of Al^{3+} ions are also discussed, which remain a significant challenge for the future development of trivalent aluminum rechargeable batteries.

Communication-Efficient Device Scheduling for Federated Learning Using Stochastic Optimization

Perazzone, Jake[1*], *Wang, S.*[2], *Ji, M.*[3], *and Chan, K.*[1]

[1]CCDC Army Research Laboratory, **FCDD-RLC-NT**, Adelphi, MD, [2]IBM, [3]Department of Electrical and Computer Engineering, University of Utah, Salt Lake City, UT

*corresponding author: jake.b.perazzone.civ@army.mil

Linear optical technology is a critical to the construction and implementation of quantum networks. A key requirement of any such system is the successful measurement of quantum states. This poses a particular challenge for linear optical systems, which are severely limited in their ability to discriminate between orthogonal entangled states. For instance, the maximally entangled Bell States can only be discriminated with a 50% success probability, when no ancillary photons are allowed. The optimal protocol is known for Bell States, but not for more general orthogonal states. The goal of our work is to give a general approach for constructing optimal discrimination protocols for any arbitrary set of orthogonal two-qubit optical states for linear optical setups with no ancillary photons. These results will hopefully lead to improving the potential result of linear optical protocols for systems where non-maximally entangled states are present.

BOLD Activity Variability as a Neural Marker of Fatigue on Sustained Alertness Tasks

Pinto, Italo'Ivo Lima Dias[1], Bansal, K.[1], and Garcia, J.[1]*

[1]CCDC Army Research Laboratory, **FCDD-RLH-FB**, APG, MD

*corresponding author: italoivo@gmail.com

The ability to maintain alertness and attention for a sustained amount of time is essential for a wide range of tasks and has severe consequences on other aspects of cognition and decision making. The psychomotor vigilance test (PVT) is one of the most used assessments of vigilance and alertness where subjects are asked to make a motor response as soon as they perceive a visual stimulus on the screen, this procedure is repeated for several minutes. From this task, alertness is associated with the response time to the briefly presented stimulus. Recently, researchers have investigated the ratio of the variability of blood oxygen level dependent (BOLD) activity between brain networks, containing somato-motor and sensory regions of the brain, and the perception of the speed of time (Northoff, G. et al. 2018). Here we probe the effects of the balance of sensory and somatomotor network activities on the performance of the subjects during the PVT in which the response time is essential. We examined the ratio of fMRI BOLD variability for visual and somatomotor networks whilst subjects were engaged in the PVT. We observed that the temporal evolution of the visual and somatomotor variability ratio decays over time and is highly correlated to the decay in performance after a brief transient period. Our results suggest that the emergence of fatigue from time-on-task can alter the visual and somatomotor balance and then affect the performance. This work presents a new avenue to assess alertness states that are crucial for emerging sensing and autonomous capabilities, supporting the complex decision-making process of humans within a multiplexed socio-technological ecosystem.

Flexible Coding of Adaptive Decision Choices in Humans and Artificial Neural Networks

Rungratsameetaweemana, Nuttida[1], Bansal, K.[1], and Garcia, J.*

[1]CCDC Army Research Laboratory, **FCDD-RLH-FB**, APG, MD

*corresponding author: nuttida.rungrat@gmail.com

A fundamental question in neuroscience and artificial intelligence concerns how adaptive decisions can be consistently and flexibly generated given the spatiotemporal complexities of naturalistic sensory information. The present study addresses this question through a complementary blend of human psychophysics, electrophysiological recordings, and deep learning. Specifically, by combining human electroencephalography (EEG) with a recurrent neural network (RNN) model, we investigate the neural mechanisms that underlie adaptive decision making under different task demands and environmental constraints. First, we propose a fundamental framework that describes the potentially differential computation that forms a basis for goal-directed decision making in humans and RNN models under several levels of sensory complexity. According to this formulation, we then construct the RNN models to be ecologically plausible and anatomically informed and

demonstrate that these models recapitulate the behavioral patterns of human participants on a dynamic visual decision task. Specifically, both humans and RNN models can successfully extract important visual features from past experiences and used them to guide their future decisions. Current efforts focus on further testing the RNN models on more complex decision tasks and comparing the underlying model dynamics to the neural (EEG) activities of humans. Together, these proposed experimental and computational frameworks provide a foundation for hybrid decision making in human-AI teaming. Insights into such processes will be critical for constructing robust human and machine hybridization that will revolutionize the direct interaction between Soldier and technology, thereby increasing the quality and effectiveness of information transfer and team understanding under different task demands.

Data-Driven Chemical Kinetic Reaction Mechanism for F-24 Jet Fuel Ignition

Ryu, Je Ir[1*] *and Kweon, C-B. M.*[1]

[1]CCDC Army Research Laboratory, **FCDD-RLC-V**, APG, MD

*corresponding author: j.ryu@anl.gov

A data-driven chemical kinetic mechanism for the military version of Jet A, F-24, is developed for numerical simulations of the ignition process. The main purpose of this study is to obtain a practical F-24 mechanism across wide temperature and equivalence ratio ranges, with a particular focus on the negative temperature coefficient and low temperature regions, for U.S. Army Unmanned Aircraft Systems (UAS) propulsion applications. The new mechanism (ARLMech-HC-F24) is based on the HyChem model of a similar fuel and optimized using a micro-genetic algorithm against an experimental ignition delay data set of the target fuel. The development and optimization processes include reaction selection, population creation, shuffled tournament implementation based on a merit function, and child-individual creation for the next generation. Several techniques and parameters are proposed to generate an accurate mechanism through an efficient process. The newly introduced data-driven mechanism based on these techniques shows better merit value convergence and represents the ignition behavior more accurately than that without the techniques. This practical mechanism is suitable for the numerical simulations of the F-24 or Jet A ignition problem, and the suggested strategies can be employed in similar problems of rate coefficients estimation.

Apparatus and Techniques for the Deployment and Characterization of Event-Based Sensors in Protection Systems

Sengupta, Jonah P.

[1]CCDC Army Research Laboratory, **FCDD-RLW-TD**, APG, MD

*corresponding author: jonah.p.sengupta.ctr@army.mil

Event-based cameras offer a passive, low-power solution to the unique needs of sensing for protection systems. However, due to the recent inception of the technology, additional work and infrastructure is needed to make current event-based sensing platforms compatible with the implementation and testing of armor devices. This work details the construction and utilization of various techniques and apparatus used to characterize and deploy event-based sensors in a testing scenario. Such apparatus includes: a custom-motor mount and programmable driver for characterizing velocity algorithms and a vertically integrated embedded platform to coordinate trigger timings of event cameras. These pieces of equipment and techniques have been demonstrated to specify latency, bandwidth, and processing capabilities in environments ranging from optical benches to active test sites. Additional work and development of these tests and instruments are needed to continue the maturation of the technology but they form a strong base for future work to build upon.

Production of Core-Shell Aluminum Nanoparticles via Scalable Atmospheric Plasma Surface Treatment and Coating

Thapa, Dinesh[1], Wu, C-C.[1], Pesce-Rodriguez, R. A.[1], Giri, L.[1], and Walck, S. D.[2]*

[1]CCDC Army Research Laboratory, **FCDD-RLW-WA**, APG, MD, [2] CCDC Army Research Laboratory, **FCDD-RLW-MC**, APG, MD

*corresponding author: dinesh.thapa.ctr@army.mil

Aluminum core shell nanoparticles (nAl) are of great interest due to their high heat of combustion and potentially rapid energy release rate enabled by their large specific surface area. Previous studies conducted at US Army Combat Capabilities Development Command Army Research Laboratory has demonstrated enhanced reactivity of the nAl after atmospheric pressure plasma surface treatment and coating using carbon monoxide as the precursor in custom-made dielectric barrier discharge (DBD) plasma reactors. Key plasma experimental conditions were identified from preliminary efforts demonstrating the capabilities of producing energetic carbon-coated nAl (nAl@C) with a ~200 mg yield per batch. Ongoing scale-up efforts have been started to produce samples in 500 mg per batch using a larger DBD reactor and characterization has demonstrated consistent structural and chemical properties as those produced by previous smaller reactors. Specifically via high resolution transmission electron microscopy (HRTEM), the resultant nAl@C samples revealed thinned oxide shell of less than 3 nm thickness with sporadic γ-Al_2O_3 deposits and a thin dispersive layer of carbonaceous coating on nAl@C surfaces. Such consistent nanoscale surface properties for the newly-produced large batch nAl indicate a great potential to produce surface-modified nAl in large quantities via atmospheric plasmas.

Determining Phase Coexistence Curves for Fully Atomistic Models of RDX and HMX

Tow, Garrett M.[1], Larentzos, J. P., and Brennan, J. K.[1]

[1]CCDC Army Research Laboratory, **FCDD-RLW-WA**, APG, MD

*corresponding author: garrett.m.tow.ctr@army.mil

When modeling an energetic material using mesoscale or continuum level simulations, material properties must be available for parameterization. One way to estimate these properties is by computing them through higher resolution simulations such as atomistic molecular dynamics, which uses a classical particle physics-based approach to describe the material. Determining thermodynamically rigorous state points at phase coexistence is challenging both computationally and experimentally due to kinetic barriers and the associated phenomena of superheating and supercooling. In my work, the pseudo-supercritical path (PSCP) method is utilized for computing the difference in the Gibbs free energy of the two coexisting phases. Using this information, the solid-liquid and solid-solid coexistence conditions for various polymorphs of RDX and HMX at a wide range of pressure conditions can be determined. Preliminary results are shown, challenges with the method are discussed, and supplementary methods for improving computational efficiency are presented.

Designing Effective Problem-Solving Teams Using Agent-Based Modeling

Turalska, Malgorzata[1], Lickorish, R.[2], de Mel, G.[2], McNally, H.[3], and Stein, S.[3]*

[1] CCDC, Army Research Lab, FCCD-ALC,MD, [2]IBM UK, [3]Department of Electronics and Computer Science, University of Southampton, Highfield, Southampton

*corresponding author: gosiatura@gmail.com

The complexity of modern military operations creates a demand for efficient collaborative decision-making and problem-solving. Additionally, as military units operate in increasingly dynamic environments, the ability to respond to changing circumstances becomes paramount for mission

success. An effective response rests on correct dissemination and transfer of information across the command-and-control structure and thus is critically linked to the network of human interactions.
In this work, we take an agent-based modeling approach to collective problem-solving. We investigate three key factors affecting the performance in collaborative environments: (1) the structure of the network used to share information between agents, (2) the search strategies adopted by agents, and (3) the complexity of problems facing the group.
We show that to avoid converging on suboptimal solutions, problem solvers require a propensity for risk-taking and the ability to learn from periodic failure. We demonstrate that there exists an optimal level of risk necessary to improve group performance. Additionally, we find that team structure has a limited impact on the efficiency of search which incorporates risk. Finally, we test the suitability of reinforcement learning algorithms to determine search protocols optimizing the collective search.

Rapid Evaluation of Metal-based Reactive Materials for Energetic Formulations Under High Heating Rates

Wainwright, Elliot R.[1] and Gottfried, J. L.[1]*

[1]CCDC Army Research Laboratory, **FCDD-RLW-WA**, APG, MD

*corresponding author: elliot.r.wainwright.civ@army.mil

Metal fuels such as Al and B are commonly used as additives to explosives and propellant formulations due to their high gravimetric and volumetric combustion enthalpy. Depending on the timescale over which these materials reaction following detonation, they have the potential to enhance a wide variety of explosive effects such as blast, fireball intensity (e.g., temperature), and Gurney energy. The ability of a given material system to react at detonation-relevant timescales can be estimated at the lab-scale prior to scale-up by measuring the shock behavior and chemical reactions in and directly following a laser-induced plasma. Here, we will discuss recent efforts to upgrade ARL's Laser-induced Air-shock from Energetic Materials (LASEM) systems, which allow for sampling of materials reactions from ~ 1 μs to 100's ms. Such a method is typically paired with a host of optical measurements to track oxidation or other reactions at the same timescales and rapidly compare novel materials to common commercial benchmarks. We present some examples of academic collaborations evaluating promising new Al and B-based fuels and the characterization of their fast energy release. The rapid assessment of these types of novel reactive materials is critical to creating new munitions and propulsion systems with enhanced speed, range, lethality, and miniaturization.

XPORT ENTRAP: A Droplet Microfluidic Platform for Enhanced DNA Transfer Between Microbial Species

Wippold, Jose A.[1], Chu, M.[1], Adams, B.[1], and Han, A.[2]*

[1]CCDC Army Research Laboratory, **FCDD-RLH-BA**, Adelphi, MD, [2]Department of Electrical and Computer Engineering, Texas A&M University, College Station, TX

*corresponding author: jose.a.wippold.civ@army.mil

A significant hurdle for the widespread implementation of synthetic biology and other genetic engineering tools into various microbes is the challenge of high throughput DNA introduction into cells. Common approaches to DNA uptake, such as competent cell transformation, electroporation, and transfection, are typically only amendable to a very small subset of laboratory bacterial strains and leaves the vast majority of microbial life genetically inaccessible. To address this challenge, we developed a novel system named DNA ENTRAP (***DNA Enhanced TRAnsfer Platform*),** which is a droplet based microfluidic platform that generates nano-bioreactors, providing the capability to streamline the development of genetic transfer. DNA ENTRAP as a system simplifies and enhances XPORT-mediated, cell-to-cell DNA transfer events using a high-throughput microfluidic approach. The system developed here, DNA ENTRAP, aims to address current limitations by circumventing the need laboratory environments, as XPORT conjugation is conducive within harsh environments.

We determined the conjugation efficiency to be superior when using DNA ENTRAP compared to the conventional benchtop method for various ratios at 0.5 hr, 1 hr, and 2 hr, respectively and delivering improvements on efficiency over an order of magnitude at certain timepoints. DNA ENTRAP has demonstrated efficient XPORT mediated nucleic acid transfer and thus establishes itself as the first system capable of screening multi-parameter conditions needed to streamline the development of genetic transfer protocols. DNA ENTRAP targets being an essential tool in the future synthesis, discovery, and development of novel organisms with potential applications in military, therapeutics, and energy.

Appendix B. Contributed Posters Presented at the 6th Postdoc and Early Career Research Day*

* The contents of this appendix appear in original form, without editorial change.

Infrared Optical-Field-Driven Luminescence in Quantum Dots

Ibrahim Boulares1, JiaoJian Shi[2], Blair C. Connelly[1] and Keith A. Nelson[2]

1 U.S. Army Research Laboratory, Sensors and Electron Devices Directorate, Adelphi, MD 20783, USA
2 Department of Chemistry, Massachusetts Institute of Technology, Cambridge, Massachusetts 02139, USA

Objective

- To investigate the fundamental properties of **optical-field-driven** electroluminescent upconversion of quantum dots (QDs) under infrared (IR) radiation

Motivation

- This study explores a potential path towards compact, low-cost, room-temperature, IR and THz detectors, and electro-optic (EO) modulators that up-convert long-wavelength signals to the visible spectral range where efficient detectors are readily available.
- A recent study of CdSe-CdS core-shell colloidal QDs under excitation from intense THz-frequency ultrafast pulses demonstrated luminescence near the visible QD bandgap [1].
- QD luminescence is associated with rapid modulation of the QD bandgap by THz electric field.
- QD luminescence is due to dot-to-dot charge transfer – ***a classical response***

Image of THz-driven luminescence (left); THz field-dependent luminescence in QD (right)

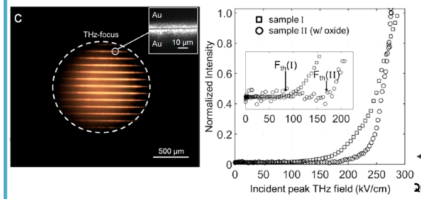

Excitation Mechanism vs Wavelength

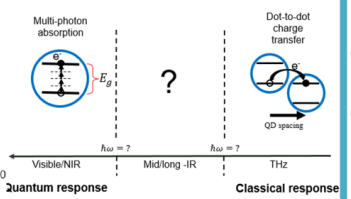

Experimental Methods

- We seek to gain a fundamental understanding of the dependence of the optical field-induced luminescence on the wavelength of the electromagnetic pulse.
  → **Does phenomenon persist as λ is decreased?**
- New experimental capability developed for study
  - Tunable pulses from 1.1 to 2.6 μm and 3.5 to 12 μm generated with an optical parametric amplifier (OPA) and difference frequency generator (DFG), respectively
  - IR pulses are focused on QDs and the visible luminescence is collected via a photomultiplier tube
  - Samples are colloidal QDs on glass
- Bright visible luminescence of commercially-available CdSe-CdS QDs driven by 10-μm IR pulses can be imaged with a commercially-available (COTS) camera
  → Demonstrates viability of application

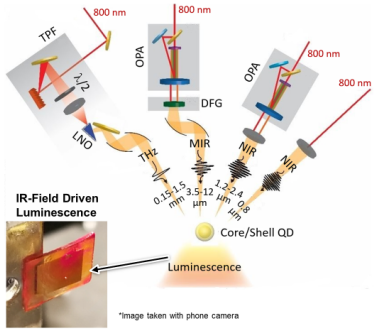

Tunable Ultrafast Laser Excitation of QDs for NIR - THz

Results

- Demonstrated IR-to-visible upconversion in various QD material → IR-induced emission from QDs at *any* sub-bandgap frequency is possible.
- Studies of QD luminescence in the mid- and long-IR (top-right figures) show a threshold, with respect to laser fluence.
  - For Red QDs, the threshold is ~2 order-of-magnitude smaller for a laser wavelength that 8 times smaller than the QD band edge (λ ≤ 4.5 μm in red QDs). → Suggests a different excitation mechanism
- Data of QD Luminescence vs. pump laser power for Blue and Red QDs in the range 0.4 to 2.2 μm shows a multi-photon behavior (quantum response), as expected. Absorption of up to 4 photons are observed in all samples.
- 5-photon absorption seen in Blue QDs in solution. We attribute the suppression of 5-photon absorption in QD arrays to dot-to-dot charge transfer between nearby dots.
- A change of the excitation mechanism occurs when the wavelength is 4 to 5 times longer than the QD emission wavelength.
- The emission decay slope (proportional to the inverse lifetime) of Red and Blue QDs arrays exhibits:
  - An increasing trend for wavelengths below the band edge, up to about 5 times the emission wavelength.
  - The decay slope then decreases as the excitation wavelength is increased.
- The observed behavior indicates:
  - Shorter excitation wavelengths result in single or multi-photon generation of excitons
  - Longer wavelengths *also* induce electroluminescence through dot-to-dot charge transfer, leading to more complex decay kinetics
- These results are consistent with the fluence dependent data of the QD luminescence.

IR field-dependent luminescence of (left) CdSe:CdS; and (right) CdS-ZnS QDs at various wavelengths

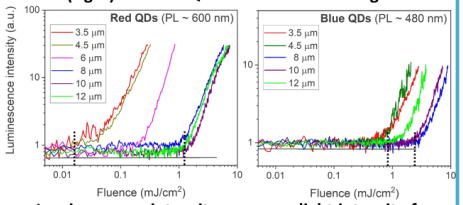

Luminescence intensity vs. pump light intensity for Red QDs (left); the slopes retrieved from linear fitting for each wavelength in the NIR (right)

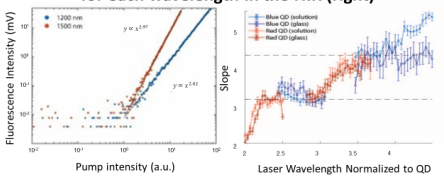

Absolute decay slopes as a function of wavelength

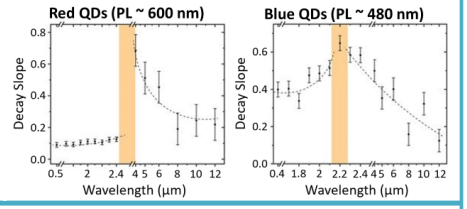

Conclusion

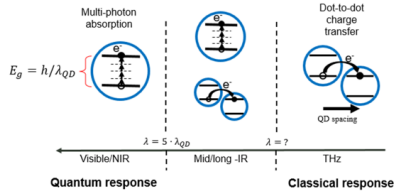

Path Forward

- Luminescence-dependence on a sub-bandgap pump to characterize the shift in the absorption edge due to the IR-fields (Stark-shift measurements).
- Incorporate field enhancement structures to lower the upconversion field threshold.

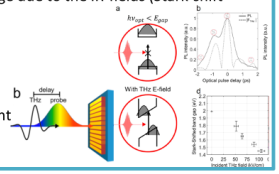

[1] B. C. Pein, et al., Nano Letters, 17, 5375 (2017).

Towards the optimal squeezed states: an optimal control approach

S.C. Carrasco[1], M.H. Goerz[1], V. Vuletić[2], and V.S. Malinovsky[1]
Email: seba.carrasco.m@gmail.com

[1]U.S. Army Research Laboratory, FCDD-RLC-NT, Adelphi, Maryland 20783, USA
[2]Department of Physics, MIT-Harvard Center for Ultracold Atoms and Research Laboratory of Electronics, Massachusetts Institute of Technology, Cambridge, Massachusetts 02139, USA

Introduction

Optical lattice clocks (OLC) operating near the standard quantum limit (SQL) employ uncorrelated atoms to reach unprecedented accuracy. The quantum noise limits the accuracy scaling to $N^{1/2}$, where N is the number of atoms. Entangled states, such as spin squeezed states (SSSs), can generate better scaling. Experimentally, these entangled states are generated by an effective one-axis twisting (OAT) Hamiltonian ($H = \chi S_z^2$), which leads to a sensitivity improvement proportional to $N^{2/3}$.

We propose a novel, short, and feasible pulse sequence that drives an ensemble of cold trapped atoms into a family of entangled squeezed states **that achieve precision scaling proportional to the number of atoms *N* (Heisenberg limit).**

Methods

First we derive analytically which is the optimal SSS for metrology given a fixed value of contrast, which are eigenvectors of

$$H = \chi S_z^2 + \lambda S_x$$

as we can show analitically. Then we use optimal control theory (OCT) to design a series of alternating S_z^2 and S_x pulses that reach this family of optimal SSSs.

Results

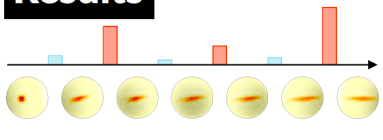

Figure 1: Schematic representation of the pulse sequence. The blue and red bars represent the shearing strength of the S_z^2 pulses and the rotation angle generated by the S_x pulses, respectively. The arrow represents time. The Bloch sphere represents the many-body entangled state as it gets squeezed over the z-direction (vertical) and anti-squeezed in the perpendicular direction (horizontal) as the pulses are applied.

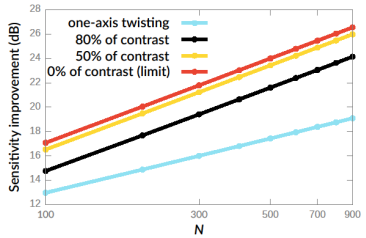

Figure 2: Comparison of the sensitivity improvement with respect to the SQL using only the OAT Hamiltonian, our pulse scheme for two contrast values, and the limit when the contrast goes to zero, corresponding to the best possible sensitivity of a standard Ramsey measurement.

Final remarks

The pulse sequence that we proposed only employs one-axis twisting Hamiltonian and standard rotation pulses. These are the same elements used to make 11.8 dB improvement beyond the SQL for N=350 atoms, the most precise interferometer to date. We estimate an improvement with our sequence of 14.9 dB beyond the SQL for the same number of atoms (considering precision losses due to experimental considerations). In the future, we would like to use our methods in other promising interferometry schemes that employ entangled states that optimize Fisher information instead of spin squeezing.

Understanding Small Molecule Interactions on Alumina Surfaces Using Reactive Molecular Dynamics Simulations

Benjamin Evangelisti[1], Chi-Chin Wu[2], Dinesh Thapa[2], Dylan Anstine[3]

1. **Penn State University Department of Chemistry, Ph.D. Candidate**
2. Weapon Sciences Division, WMRD, DEVCOM-ARL
3. University of Florida, Department of Mat. Sci. Eng.

Background

Aluminum (Al) nanoparticles (nAl) can potentially resolve issues of larger Al energetic materials if their parasitic alumina shells can be mitigated. Preliminary experiments have demonstrated that an aluminum carboxylate/aluminum hydroxide coating on surface-modified nAl with a reduced alumina shell thickness leads to enhanced energetic performance. Characterization of this coating is still the subject of ongoing research and can benefit from atomistic-scale simulations.

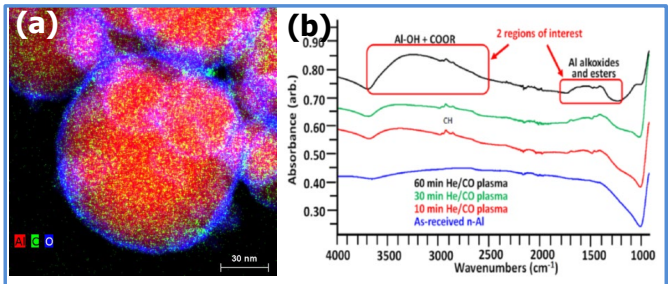

TEM mapping of carbon coating (a) identified as aluminum hydroxides and carboxylates by FTIR by ARL researchers [1] (b).

Objective

Provide insights into the formation of carbon coating on surface-modified nAl by studying the dehydrogenation reactions of alumina-surface-adsorbed CH_4, H_2O, and HCOOH using reactive molecular dynamics (MD) simulations.

Investigated Species

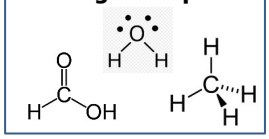

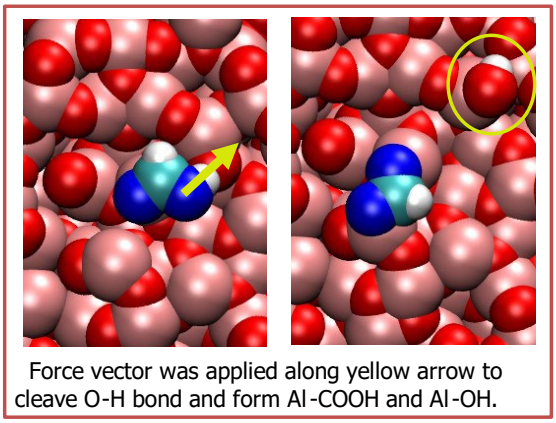

Force vector was applied along yellow arrow to cleave O-H bond and form Al-COOH and Al-OH.

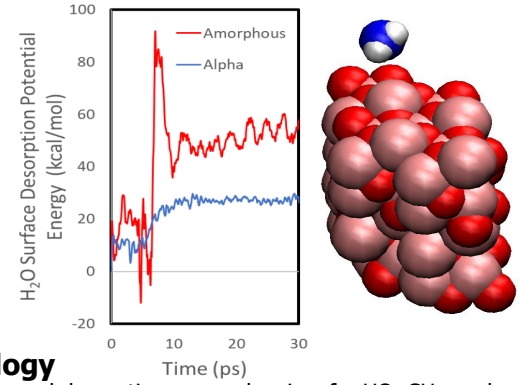

Methodology

The adsorption and desorption energy barriers for H_2O, CH_4, and HCOOH on the alpha (α) alumina and amorphous alumina surfaces were measured using reactive MD simulations by usingReaxFF bond restraints to move molecules towards or away from the alumina surface. Barriers were identified from the MD potential energy.

Dehydrogenation barriers for surfaceadsorbed H_2O, CH_4, and HCOOH were measured using reactive MD simulations by using a weak bond restraint to keep the molecule on the alumina surface while a strong bond restraint caused the C-H or O-H bond to dissociate.

Key Results

The dehydrogenation barrier was, on average, 10 kcal/mol lower than the desorption barrier for CH_4, H_2O, and HCOOH on the amorphous alumina surface indicating that dehydrogenation can occur without molecules leaving the surface. The dehydrogenation barriers for H_2O and HCOOH on the α-alumina surface were found to be higher than the corresponding desorption barriers indicating that molecules are likely to desorb before dehydrogenation can occur.

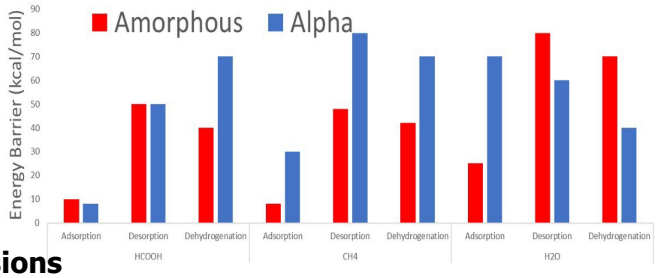

Conclusions

Dehydrogenation of surface-adsorbed small molecules provides insight into possible formation mechanisms of Al-COOH and Al-OH in support of experimental findings.

Acknowledgement

High-Performance Internship (HIP) program
ARL 2021 Summer Student Experience (HIP-21-004)

Reference

1. Wu *et al., J. of Appl. Phys.* 129, 063301, 2021.

A generalized approach to two qubit linear-optical state analyzers

Dov Fields [1 2] János Bergou [1] Mark Hillery [1] Vladimir Malinovsky [2]

[1]Hunter College, New York, NY

[2]US Army Research Laboratory, Adelphi, MD

Abstract

Linear optical technology is a critical to the construction and implementation of quantum networks. A key requirement of any such system is the successful measurement of quantum states. This poses a particular challenge for linear optical systems, which are severely limited in their ability to discriminate between orthogonal entangled states. For instance, the maximally entangled Bell States can only be discriminated with a 50% success probability, when no ancillary photons are allowed. The optimal protocol is known for Bell States, but not for more general orthogonal states. The goal of our work is to give a general approach for constructing optimal discrimination protocols for any arbitrary set of orthogonal two-qubit optical states for linear optical setups with no ancillary photons. These results will hopefully lead to improving the potential result of linear optical protocols for systems where non-maximally entangled states are present.

Linear Optical Systems

Linear optical setups use a few basic elements: beam splitters, phase shifters, and single photon detectors. These elements can be combined to create general transformations between the input modes and the output modes. In general, any unitary transformation between input and output modes ($\hat{b}_i^\dagger = \sum_j U_{ij}\hat{a}_j^\dagger$) can be realized.

Figure 1. Basic linear optical element with two input ports and two output ports. Outputs are detected by single photon deetectors.

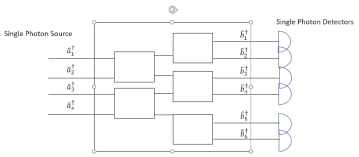

Figure 2. Linear optical elements can be combined to create more complicated transformations between input and output photons

Dual Rail Representation

The Hilbert space for photonic systems is the Fock space, which describes the total number of photons present in each possible mode. One way to define qubits in this space is via the dual rail representation:

$$\text{Fock state}: |n_m\rangle \equiv \frac{(\hat{a}_m^\dagger)^m}{\sqrt{n!}}|0\rangle$$

$$\text{Qubits}: \begin{cases} |0\rangle &= \hat{a}_1^\dagger|0\rangle \\ |1\rangle &= \hat{a}_2^\dagger|0\rangle \end{cases} \quad 2\text{ Qubits}: \begin{cases} |00\rangle &= \hat{a}_1^\dagger\hat{a}_3^\dagger|0\rangle \\ |01\rangle &= \hat{a}_1^\dagger\hat{a}_4^\dagger|0\rangle \\ |10\rangle &= \hat{a}_2^\dagger\hat{a}_3^\dagger|0\rangle \\ |11\rangle &= \hat{a}_2^\dagger\hat{a}_4^\dagger|0\rangle \end{cases}$$

Bell-like State Discrimination

Bell-like States:

- $|\Psi_1\rangle = \left(\sin\theta_1\hat{a}_1^\dagger\hat{a}_3^\dagger + \cos\theta_1\hat{a}_2^\dagger\hat{a}_4^\dagger\right)|0\rangle$
- $|\Psi_2\rangle = \left(\cos\theta_1\hat{a}_1^\dagger\hat{a}_4^\dagger - \sin\theta_1\hat{a}_2^\dagger\hat{a}_3^\dagger\right)|0\rangle$
- $|\Psi_3\rangle = \left(\sin\theta_2\hat{a}_1^\dagger\hat{a}_3^\dagger + \cos\theta_2\hat{a}_2^\dagger\hat{a}_4^\dagger\right)|0\rangle$
- $|\Psi_4\rangle = \left(\cos\theta_2\hat{a}_1^\dagger\hat{a}_3^\dagger - \sin\theta_2\hat{a}_2^\dagger\hat{a}_4^\dagger\right)|0\rangle$

Measurement:

$$\begin{pmatrix}\hat{b}_1^\dagger \\ \hat{b}_3^\dagger\end{pmatrix} = \begin{pmatrix}\cos\phi & \sin\phi \\ -\sin\phi & \cos\phi\end{pmatrix}\begin{pmatrix}\hat{a}_1^\dagger \\ \hat{a}_3^\dagger\end{pmatrix}$$

$$\begin{pmatrix}\hat{b}_2^\dagger \\ \hat{b}_4^\dagger\end{pmatrix} = \frac{1}{\sqrt{2}}\begin{pmatrix}1 & 1 \\ -1 & 1\end{pmatrix}\begin{pmatrix}\hat{a}_2^\dagger \\ \hat{a}_4^\dagger\end{pmatrix}$$

Outcomes:

In/Out	$P(1,1)$	$P(2,2)$	$P(3,3)$	$P(4,4)$	$P(1,2)$	$P(1,3)$	$P(1,4)$	$P(2,3)$	$P(2,4)$	$P(3,4)$
$\|\Psi_1\rangle$	$\frac{\cos^2\theta_1\sin^2(2\phi)}{2}$	$\frac{\sin^2\theta_1}{2}$	$\frac{\cos^2\theta_1\sin^2(2\phi)}{2}$	$\frac{\sin^2\theta_1}{2}$	0	$\cos^2\theta_1\cos^2(2\phi)$	0	0	0	0
$\|\Psi_2\rangle$	$\frac{\sin^2\theta_1\sin^2(2\phi)}{2}$	$\frac{\cos^2\theta_1}{2}$	$\frac{\sin^2\theta_1\sin^2(2\phi)}{2}$	$\frac{\cos^2\theta_1}{2}$	0	$\sin^2\theta_1\cos^2(2\phi)$	0	0	0	0
$\|\Psi_3\rangle$	0	0	0	0	$\frac{\cos^2(\theta_2-\phi)}{2}$	0	$\frac{\cos^2(\theta_2+\phi)}{2}$	$\frac{\sin^2(\theta_2-\phi)}{2}$	0	$\frac{\sin^2(\theta_2+\phi)}{2}$
$\|\Psi_4\rangle$	0	0	0	0	$\frac{\sin^2(\theta_2-\phi)}{2}$	0	$\frac{\sin^2(\theta_2+\phi)}{2}$	$\frac{\cos^2(\theta_2-\phi)}{2}$	0	$\frac{\cos^2(\theta_2+\phi)}{2}$

Table 1. The output probability $P(m,m)$, the probability of measuring one photon the the n output mode and one photon in the m output mode, is given for each input state. The highlited columns are the outputs that can contribute to unambiguous discrimination.

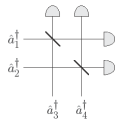

Figure 3. A diagram of the setup used to discriminate between the bell-like states.

Distinguishability of Bell-like states

Distinguishability:

$$D(m,n) = \frac{2\max_i\{P(m,n|\,|\psi_i\rangle)\}}{\sum_i P(m,n|\,|\psi_i\rangle)} - 1$$

$$D_1 = \sqrt{1-C_1^2}$$

$$D_2 = |\sqrt{1-C_2^2}\cos(2\phi) + C_2\sin(2\phi)\,|$$

$$D_3 = |\sqrt{1-C_2^2}\cos(2\phi) - C_2\sin(2\phi)\,|$$

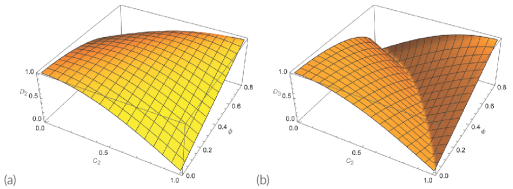

Figure 4. A plot of distinguishability (a) D_2 and (b) D_3 as a function of the concurrence C_2 and the beam splitter parameter ϕ.

Optimal Unambiguous Discrimination $\phi = \theta_2$:

In/Out	$P(1,1)$	$P(2,2)$	$P(3,3)$	$P(4,4)$	$P(1,2)$	$P(1,3)$	$P(1,4)$	$P(2,3)$	$P(2,4)$	$P(3,4)$
$\|\Psi_1\rangle$	$\frac{\cos^2\theta_1\sin^2(2\theta_1)}{2}$	$\frac{\sin^2\theta_1}{2}$	$\frac{\cos^2\theta_1\sin^2(2\theta_2)}{2}$	$\frac{\sin^2\theta_1}{2}$	0	$\cos^2\theta_1\cos^2(2\theta_2)$	0	0	0	0
$\|\Psi_2\rangle$	$\frac{\sin^2\theta_1\sin^2(2\theta_2)}{2}$	$\frac{\cos^2\theta_1}{2}$	$\frac{\sin^2\theta_1\sin^2(2\theta_2)}{2}$	$\frac{\cos^2\theta_1}{2}$	0	$\sin^2\theta_1\cos^2(2\theta_2)$	0	0	0	0
$\|\Psi_3\rangle$	0	0	0	0	$\frac{1}{2}$	0	$\frac{\cos^2(2\theta_2)}{2}$	0	0	$\frac{\sin^2(2\theta_2)}{2}$
$\|\Psi_4\rangle$	0	0	0	0	0	0	$\frac{\sin^2(2\theta_2)}{2}$	$\frac{1}{2}$	0	$\frac{\cos^2(2\theta_2)}{2}$

Table 2. The output probability $P(n,m)$, the probability of measuring one photon the the n output mode and one photon in the m output mode, is given for each input state using the optimal strategy. The highlited columns are the outputs that contribute to unambiguous discrimination.

References

[1] C. H. Bennett, G. Brassard, C. Crépeau, R. Jozsa, A. Peres, and W. K. Wootters, "Teleporting an unknown quantum state via dual classical and einstein-podolsky-rosen channels," *Phys. Rev. Lett.*, vol. 70, pp. 1895–1899, Mar 1993. [Online]. Available: https://link.aps.org/doi/10.1103/PhysRevLett.70.1895

[2] S. L. Braunstein and A. Mann, "Measurement of the bell operator and quantum teleportation," *Phys. Rev. A*, vol. 51, pp. R1727–R1730, Mar 1995. [Online]. Available: https://link.aps.org/doi/10.1103/PhysRevA.51.R1727

[3] N. Lütkenhaus, J. Calsamiglia, and K.-A. Suominen, "Bell measurements for teleportation," *Phys. Rev. A*, vol. 59, pp. 3295–3300, May 1999. [Online]. Available: https://link.aps.org/doi/10.1103/PhysRevA.59.3295

[4] L. Vaidman and N. Yoran, "Methods for reliable teleportation," *Phys. Rev. A*, vol. 59, pp. 116–125, Jan 1999. [Online]. Available: https://link.aps.org/doi/10.1103/PhysRevA.59.116

[5] J. Calsamiglia and N. Lütkenhaus, "Maximum efficiency of a linear-optical bell-state analyzer," *Applied Physics B*, vol. 71, pp. 67–71, 2001.

dovfields@gmail.com

Frequency Scaling of Passive Voltage Gain in 1-port Quartz Resonators

M. Galanko[1], S. S. Bedair[1], T. M. Kiebala[1,2], D. A. Diamond[3], R. Rudy[4], V. F.-G. Tseng[1]
Email: mary.e.galanko.civ@army.mil

[1]DEVCOM Army Research Laboratory, FCDD-RLS-CC, Adelphi, MD, 20783, USA
[2]Department of Mechanical Engineering, Rochester Institute of Technology, Rochester, NY, 14623, USA
[3]Department of Electrical and Microelectronic Engineering, Rochester Institute of Technology, Rochester, NY, 14623, USA
[4]DEVCOM Army Research Laboratory, FCDD-RLS-SA, Adelphi, MD, 20783, USA

Objective:

Provide the Army with near-zero-power "wake-up" radios that **monitor contested environments** for RF signals, continuously for a period of months to years, **without the need to replace a battery**.

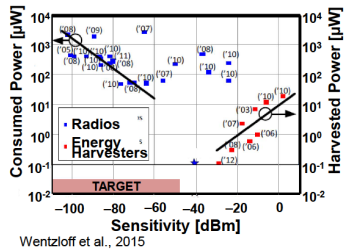

Wentzloff et al., 2015

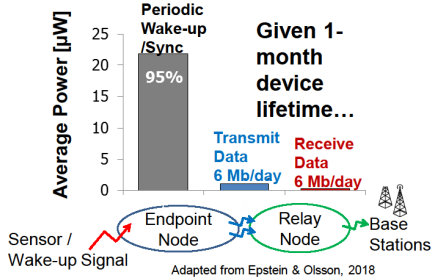

Adapted from Epstein & Olsson, 2018

Quartz Front-end Modeling

- Source/antenna + modified Butterworth van Dyke (mVBD) model + load

$$\text{Gain } [V/V]: \left|A_v\right|_{\omega=\omega_r} \approx \frac{|Z_L|}{Z_0 + \text{Re}\{Z_r\} + \text{Re}\{Z_L\}}$$

- R_m and $|A_v|$ depend upon:
  - **Device properties:** $k_{eff}^2 \times Q_m$
  - **Design parameters:** f_r, C_0

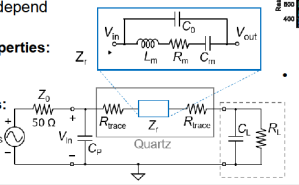

- Gain $|A_V|$ maximized at lower frequencies
- **$|A_V|$ > 40 V/V achievable at 200 MHz**

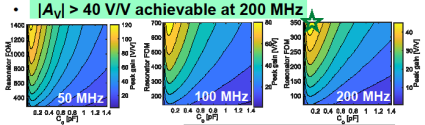

- High gain $|A_V|$ **does not require close matching** between C_0 and Z_L

For C_L = 120 fF and R_L ≈ 10 MΩ:

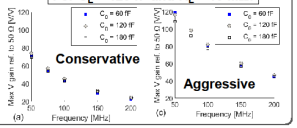

Approach:

Explore quartz as a material for low-power piezoelectric transformers (PTs)

- Investigate achievable **passive voltage gain, quality factor (*Q*), and matching** to 50 Ω
- Explore advantages of "stacking" multiple quartz substrates
- Integrate with state-of-the-art circuit with power consumption **<10 nW** for sensitivity approaching **–100 dBm**

Traditional receiver (mW):

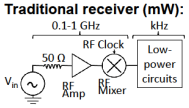

Typical wake-up receiver (nW):

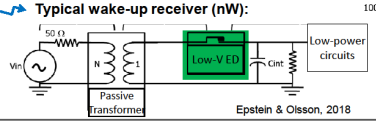

Epstein & Olsson, 2018

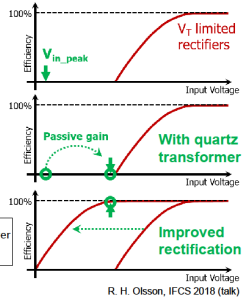

R. H. Olsson, IFCS 2018 (talk)

Results: Performance vs. Frequency, Various Designs

- **Gain up to 317 V/V - state-of-the-art**
  - Gain at high-impedance load exceeds expectations; limited by testbed Q_{elec}

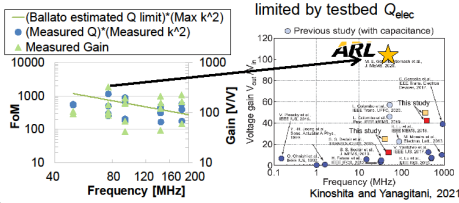

- **Loaded voltage gain exceeds conservative simulations**

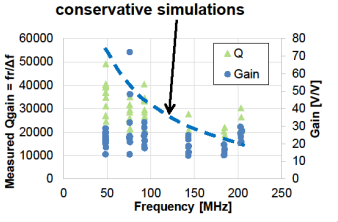

Quartz Resonator Design

Using an established technology in a new way

- Commercially available custom process
- Quartz thickness-shear mode – **high *Q***
  - Create resonant cavity for "trapped-energy mode" standing wave

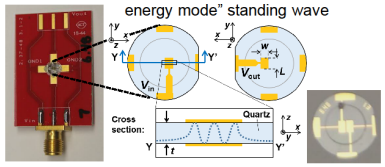

Voltage Gain Testbed

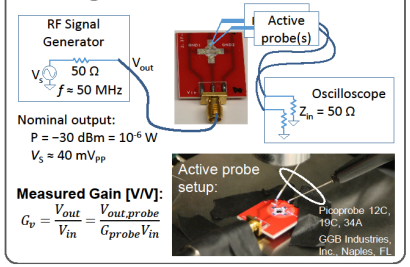

Nominal output:
P = −30 dBm = 10^{-6} W
V_S ≈ 40 mV_{PP}

Measured Gain [V/V]:

$$G_v = \frac{V_{out}}{V_{in}} = \frac{V_{out\_probe}}{G_{probe} V_{in}}$$

Results: Performance vs. Frequency, Fixed C_0, R_L

Study of **4 devices with $C_0 \approx C_L$** (±50%), AR = 1.5

- At high $Q_{elec,load}$, **high gain achievable at up to 200 MHz**
- Decay in gain with frequency is minimal at lower Z_L

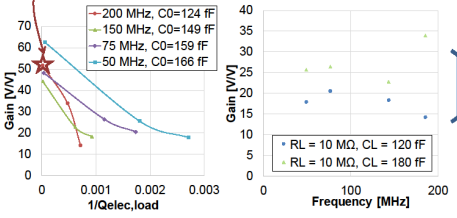

Conclusions:

- Analytical models validated and refined
- Quartz resonators are integrable with circuits with realistic input impedance (10 MΩ || 120-180 fF)
  - Uses smaller, longer-lived battery
  - **Applications:** ultra-low-power handheld radios, unattended sensors, "Internet of Things"

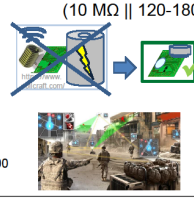

Learning through Dialogue for Soldier-Robot Interaction

Felix Gervits

Overview

Goal: Develop an approach to automated question generation for robot **dialogue-based learning** in novel environments.

Create proof-of-concept demonstration where a robot learns to perform a collaborative tool organization task.

Applications:
- scouting
- transport
- search & rescue
- etc.

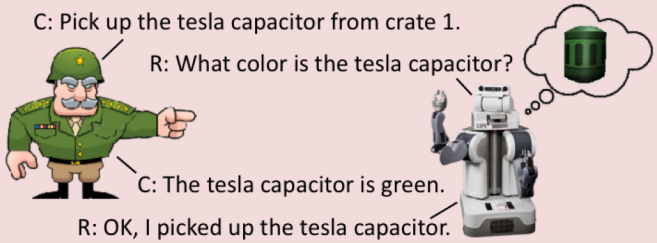

Experimental Setup

Robot in Unity 3D environment

Task: Tool organization.

Approach: Situated dialogue with remote Commander.

Challenge: Learning novel concepts.

System Architecture

Questions selected using dynamically-generated decision network.

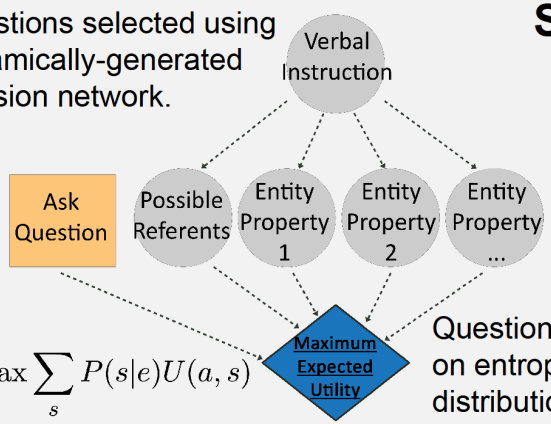

$$\operatorname{argmax}_a \sum_s P(s|e)U(a,s)$$

Question utilities based on entropy of property distributions.

Integration of the decision network with DIARC cognitive robotic architecture.

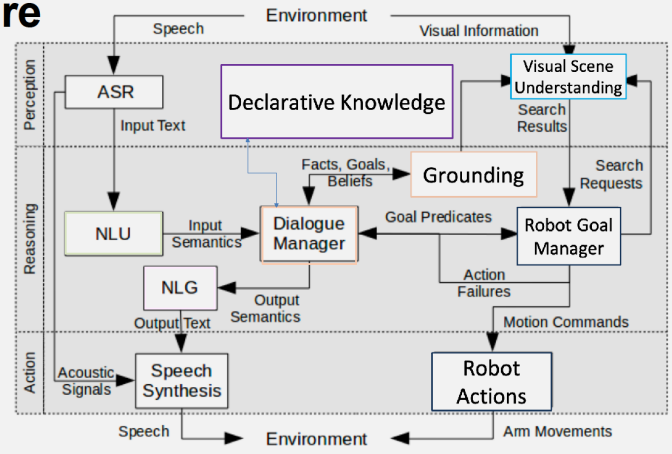

DIARC: Distributed Integrated Affect Reflection Cognition Architecture

- Demonstration shows that automated question generation is effective for learning in novel environments with little training data.

Toward Uncertainty Aware Quickest Change Detection

James Zachary Hare and Lance Kaplan

Motivation

- A sensor collects i.i.d. observations sequentially, $X_1, \dots, X_T$
- Observations are initially drawn from a distribution $P_0(X|\theta_0)$, i.e., $X_1, \dots, X_\gamma \sim P_0(X|\theta_0)$
- At some point γ the distribution of observations change to $P_1(X|\theta_1)$, i.e., $X_{\gamma+1}, \dots, X_T \sim P_1(X|\theta_1)$
- γ is the assumed unknown change point

Objective

Develop a test statistic that detects a change in distribution with a minimum delay subject to a maximum false alarm rate

Relevance

- Situational awareness of the operating environment
- Quick detection of changes is essential for C2 and defense.

State-of-the-art Approaches

$$\tau_c = \inf\{T \geq 1 | S_T > \lambda\}$$

$$S_T = argmax_{1 \leq k \leq T} \frac{\prod_{i=1}^{k-1} P_0(X_i|\theta_0) \prod_{i=k}^{T} P_1(X_i|\theta_1)}{\prod_{i=1}^{T} P_0(X_i|\theta_0)}$$

- CuSum Algorithm:
  - Assumes that both the pre- and post-change distributions are known
- Generalized Likelihood Ratio (GLR):
  - Assumes that either (1) both the pre- and post-change distributions are unknown or (2) the post-change is unknown

Current Limitations

- The parameters of the distributions are known precisely or completely unknown
- Limited knowledge of the parameters based on limited training data is not considered

Uncertain Likelihood Ratio (ULR) Test

- Assume we have a set of prior evidence (training data) for both the pre - and post-change distributions
  - $r_0 = \{r_{10}, \dots, r_{|r_0|0}\}$, where $|r_0| \geq 0$ and $r_{m0} \sim P_0$
  - $r_1 = \{r_{11}, \dots, r_{|r_1|1}\}$, where $|r_1| \geq 0$ and $r_{m1} \sim P_1$
- The parameters θ_0 and θ_1 are known within a distribution (conjugate prior)

$$f(\theta|r_0) = \frac{\prod_{i=1}^{|r_0|} P_0(r_{i0}|\theta)\, f_0(\theta)}{\int \prod_{i=1}^{|r_0|} P_0(r_{i0}|\theta)\, f_0(\theta) d\theta}$$

$$S_T^{ULR} = argmax_{1 \leq k \leq T} \left(\frac{\hat{P}_0(X_{1:k-1}|r_0) \hat{P}_1(X_{k:T}|r_1)}{\hat{P}_0(X_{1:T}|r_0)} \right)$$

- Where $\hat{P}(X|r) = \int_{\theta \in \Theta} \prod P(X|\theta) f(\theta|r) d\theta$ is a posterior predictive distribution

Relationship between ULR and GLR

- GLR estimates θ_0 and θ_1 based on the Maximum Likelihood estimates
- For Gaussian distributions and a Jeffrey's prior

$$S_T^{ULR}(k) = C \times S_T^{GLR}(k)$$

- A non-Jeffrey's prior results in θ_0 and θ_1 to be estimated based on the Maximum A Posterior estimate instead

Results

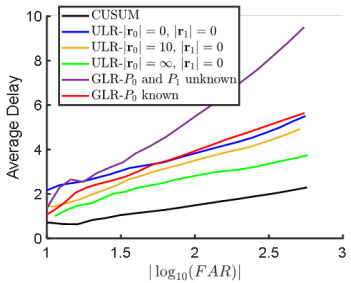

Average delay vs False Alarm Rates when the post-change distribution is unknown

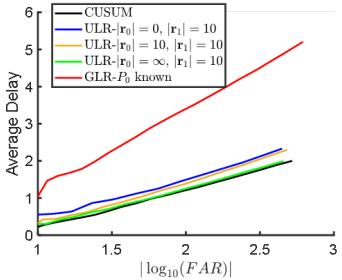

Average delay vs False Alarm Rates with prior evidence for the post-change distribution

- The ULR outperforms the GLR test statistic
- Prior evidence for the post-change distribution results in the ULR performing like the CuSUM algorithm

Future Work

- Test the ULR on IoBT MSA test bed
- Identify theoretical guarantees
- Extend to multi-agent systems

Catalytic Oxidation of Propane over Platinum Palladium Alloyed with Nickel: An Assessment of the Chemical and Intermediate Species

Haval Kareem,[1] Alex Langrock,[1] Luther Mahoney[1], Jeffery Auletta,[1] Hyun Kim,[1] Chi K. Nguyen,[2] David Mackie,[1] and Dat T. Tran[1]

1-Sensors and Electron Devices Directorate, CCDC Army Research Laboratory, Adelphi, MD 20783, USA

2-Department Of Chemistry and Life Science, United State Military Academy, West Point, NY 10996, USA

Introduction

- Volatile organic compounds including propane and CO are main constitutes of exhaust emission from military bases and infantry armored vehicles
- With growing environmental and health concerns, catalytic removal of such harmful gases is considered more efficient way than thermal decomposition
- Understanding the correlation of the atomic structures and the catalytic synergy remains a highly challenging task for the design of active and robust oxidation catalysts
- The combination of in situ experimental techniques, synchrotron high-energy X-ray diffraction coupled to atomic pair distribution function (HE-XRD/PDF) and DRIFTS (Diffuse Reflectance Infrared Fourier Transform Spectroscopy) is a powerful method to understand the catalytic synergy of nanoalloy catalysts by investigating alloying phase structure, probing surface intermediate species and reaction mechanism under real reaction conditions

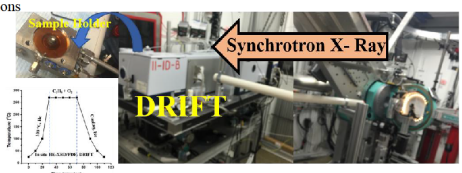

In Situ combination of HE-XRD/PDF/DRIFT

Morphology

- Average sizes of $Pt_{18}Pd_{63}Ni_{19}$, $Pt_{17}Pd_{42}Ni_{41}$, and $Pt_{16}Pd_{16}Ni_{68}$ NPs are 5.8 ±1.7 nm, 8.6±2.2 nm and 7.7±2.9 nm respectively
- Uniform distributions of the three metals across the NPs
- No indication of phase segregation

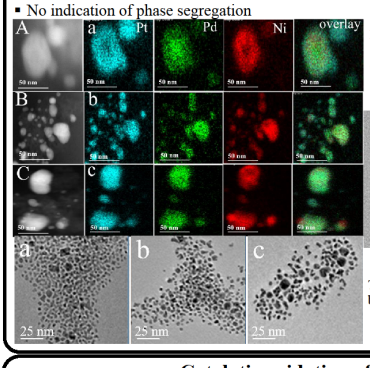

HAADF-STEM and the EDX for supported Al_2O_3 supported (A)$Pt_{18}Pd_{63}Ni_{19}$ nanoparticles; (B) $Pt_{17}Pd_{42}Ni_{41}$;(C) $Pt_{16}Pd_{16}Ni_{68}$.

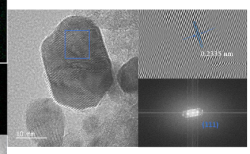

The lattice fringe features 0.2335 nm falls in between Pt and Pd NPs[1]

Catalytic oxidation of propane

- The catalytic activity in order of $Pt_{16}Pd_{16}Ni_{68} > Pt_{17}Pd_{42}Ni_{41} > Pt_{18}Pd_{63}Ni_{19}$
- T_{10} and T_{50} shows a minimum value at composition of ~50% Ni
- The E_a for $Pt_{16}Pd_{16}Ni_{68}$ exhibited the smallest value (39 kJ/mol)[2, 3]

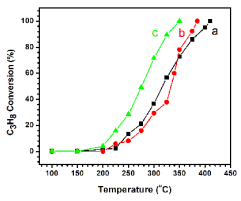

$Pt_{18}Pd_{63}Ni_{19}$ (a, black), $Pt_{17}Pd_{42}Ni_{41}$ (b, red), and $Pt_{16}Pd_{16}Ni_{68}$ (green)

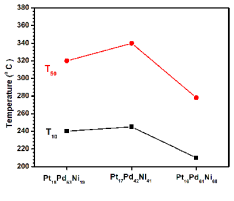

T_{10}, T_{50} as function of composition

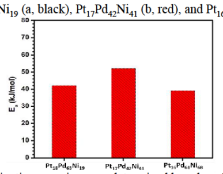

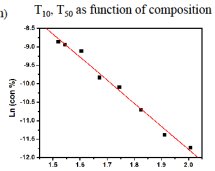

Activation energies were determined based on Arrhenius plot

In-situ HE-XRD/PDF

- The atomic arrangement fits well with the FCC alloy structure during all the sequences of treatments
- Presence of well-structured metallic oxide layers characteristic to NiO and PtO phases
- The lattice parameters of the PtPdNi /Al_2O_3 catalysts were extracted from the experimental PDF data

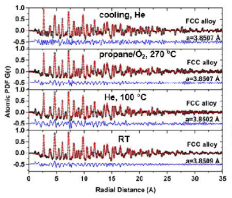

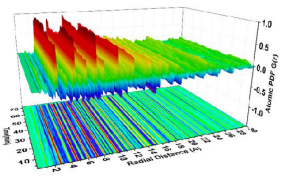

(left)In-situ PDFs for $Pt_{16}Pd_{16}Ni_{68}$ catalysts. Experimental data (symbols in black), and fit model (line in red) of the total atomic PDFs. (right) 3D PDF color map

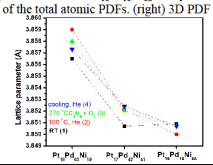

catalysts shows reduction and expansion of lattice parameter based on treatment environment

Combined In situ HE-XRD/PDF/DRIFT

- Intensity of intermediate species depends on NPs composition
- Atomic structural changes in line with intermediate species growth over PtPdNi/ Al_2O_3
- The intensities of the bands become stronger on NPs with Ni > 40%
- Formate and bicarbonate were not detected on NPs with Ni < 40%

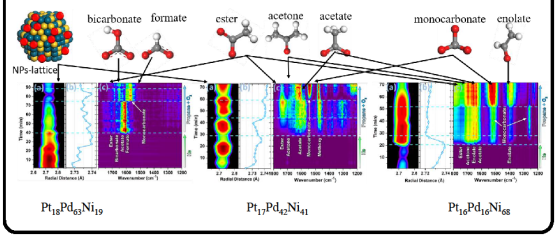

$Pt_{18}Pd_{63}Ni_{19}$ $Pt_{17}Pd_{42}Ni_{41}$ $Pt_{16}Pd_{16}Ni_{68}$

CONCLUSIONS

- Alloying PtPd with Ni with an optimal composition can enhance the catalytic activity for propane oxidation
- Strong composition dependence of the catalytic activity
- Atomic structural changes depend on catalyst composition and reaction condition
- The absence of adsorbed formate and bicarbonate species Ni ~ 40 % PtPdNi alloy is linked to the higher activity in terms of achieving a complete C-C cleavage

Path Forward/Acknowledgment

- Investigations of nanoparticles, nanowire, nanotube catalysts in terms of size, shape, composition, and surface properties for gas phase reaction
- Comprehensive computational modeling to gain further insights into the structure-activity correlation

❖ CJ Zhong Research Group members

❖ Work and access to Beamline 11-ID-C at the Advanced Photon Source was supported by the U.S. Department of Energy (DOE) Office of Science

REFERENCES

1. M. Baldi, E. Finocchio and F. Milella, *Appl. Catal., B*, 1998, **16**, 43-51.
2. C.-H. Lai, C.-C. Chang, C.-H. Wang, M. Shao, Y. Zhang and J.-L. Wang, *Atmos. Environ.*, 2009, **43**, 1456-1463.
3. S. C. Kim and W. G. Shim, *Appl. Catal., B*, 2009, **92**, 429-436.

SURFACE-DISPLAY TECHNIQUES TO EXPLORE INTERFACIAL INTERACTIONS OF NON-POLAR SUBSTRATES

Mark T. Kozlowski*, Joshua A. Orlicki, Randi M. Pullen
* mark.t.kozlowski4.civ@army.mil, 410-306-0297

Outline

In this work, we display fungal proteins known as hydrophobins on the surface of bacterial cells, then screen to see if doing so makes the cells more adhesive to polymers of interest. On-cell screening is cheaper than testing recombinant protein directly, and allows for easy modification of the protein as part of an optimization process.

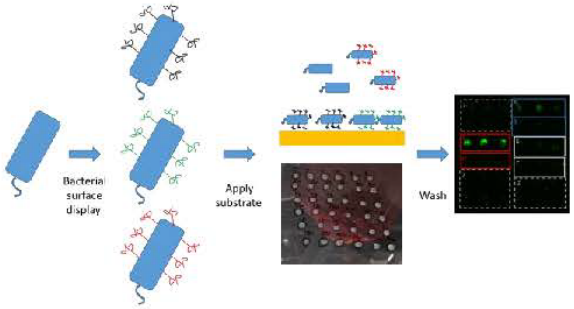

For a more complete version of this work, see ARL-TR-9312 (SEP 2021)

What our constructs look like

The constructs are displayed using the Autotransporter surface display system. A surface display protein is embedded in the bacterial outer membrane. N-terminal to this protein is the hydrophobin of interest, as well as a 6xHistidine epitope tag. Successful display can be confirmed using an antibody that targets this tag, and which is conjugated to a fluorescent dye. Successful surface display results in fluorescent cells, which can be measured by flow cytometry.

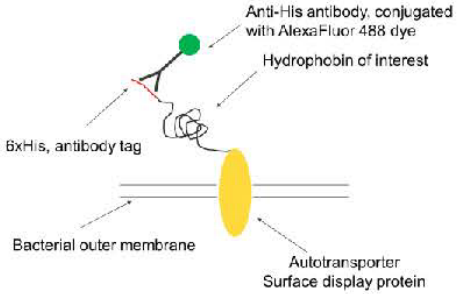

Hydrophobin display confirmed by flow cytometry

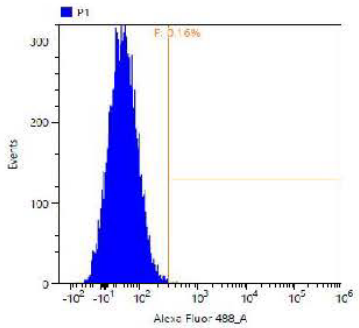

Uninduced

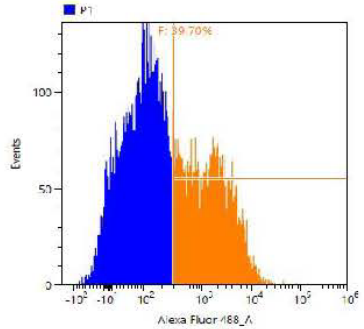

Induced

Flow cytometry indicates successful display of hydrophobins such as NC2 (shown here). If surface expression is turned off (uninduced), the population of observed cells is not fluorescent. However, if the protein is expressed, a population of fluorescent cells can be observed (induced). As shown in "what our constructs look like", this fluorescence indicates the presence of the hydrophobin of interest.

Display promoted bacterial adhesion to polymers

After confirming surface display, the hydrophobin constructs were put into fluorescent bacterial cells. 100uL of cells were spotted into polymers of interest, either after having expression induced (boxes A, C, and E) or suppressed (boxes B, D, and F). After a wash step, a fluorescent image is taken. If the cells stick to the polymer of interest, a fluorescent residue should be left behind. Gratifyingly, these residues are observed only when hydrophobin expression is on, and not when it is suppressed, suggesting the specific hydrophobins studied (NC2, DEW, Sc3) promote bacterial adhesion.

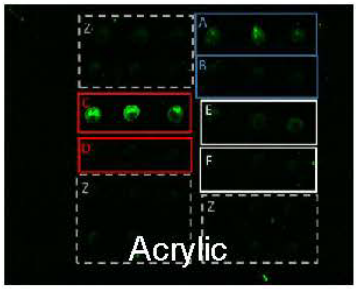

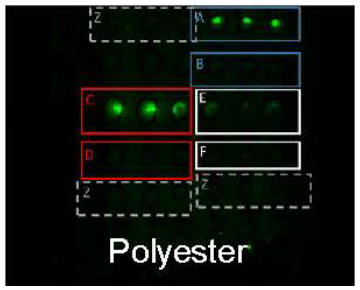

Production of Highly-Crystalline, Free-Standing, Imine-Based 2D Polymer Films

Presented at the 6th Annual ARL Postdoc and Early Career Research Symposium - September 22, 2021
POC: David C. McLeod*, Contributors: Morgan G. Barnes and Robert H. Lambeth
*david.c.mcleod2.civ@army.mil, Composite and Hybrid Materials Branch, DEVCOM Army Research Laboratory, APG, MD

Background / Previous Work

Imine-based 2D polymers are porous, sheet-like molecules that could be useful in a wide variety of applications, such as gas separation and water purification membranes, supports for catalysts and sensors, components in batteries and biomedical devices, and as tough engineering materials.

Current techniques produce aggregated polycrystalline powders or nm-thickness films that cannot be dissolved or melted in large quantities for processing into more-useful, mechanically-robust form factors, such as large-area, micron-thickness films.

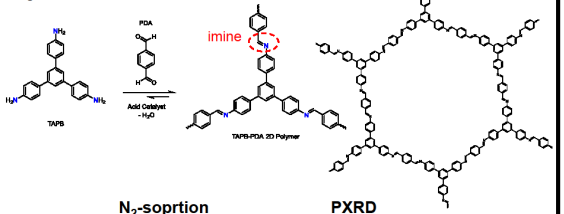

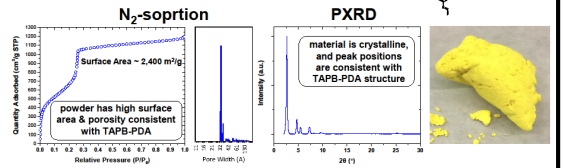

Dissolving 2D Polymer in Acid/Water Mixture, Drop-Casting

- Powdered 2D polymers are difficult to dissolve because of cross-linking between distinct molecular sheets.
- Imine bonds can be broken in the presence of water and an acid catalyst. Adding a small amount of H_2O with an acid breaks some imine bonds, dissolving, but not completely depolymerizing, the 2D polymer.
- Upon casting and evaporation of acid/H_2O, the imine bonds will reform, and the 2D polymer will solidify into a continuous film.

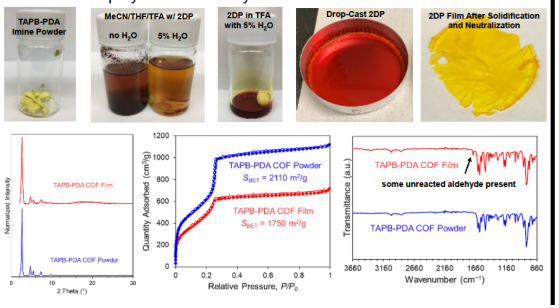

Creating Higher Quality 2DP Films

Motivation: In previous work, a new method for producing micron-thickness films from imine-based 2D polymer powders dissolved in TFA/water was developed, but the resulting films had significantly lower crystallinity than powders, and results were inconsistent from run to run. Drop-casting also produced films of non-uniform thickness.

Strategy to Improve Film Quality: Doctor blading is generally a better method for producing films of uniform thickness. In 2D polymer powders, longer reaction times at higher temperatures result in greater crystallinity, because the imine bond is reversible, and imine-exchange reactions can also happen, in the presence an acid catalyst. Imine bonds will continuously break and reform, improving the molecular perfection of the polymers.

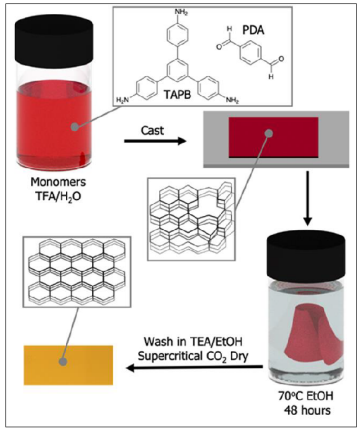

Casting and post-film formation processing procedure to obtain highly-crystalline 2D polymer films.

1. Monomers (TAPB and PDA) are dissolved in a TFA/water solution and are doctor-bladed to form a uniform film.
2. After solidification, the film is then heated in ethanol, with residual TFA still present, for 2 days at 70ºC.
3. The film is neutralized in a triethylamine (TEA) and ethanol solution, and super-critical CO_2 dried to give a crystalline film.

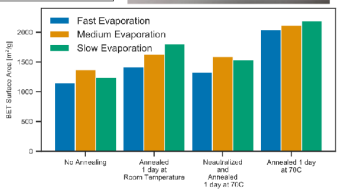

Film Characterization

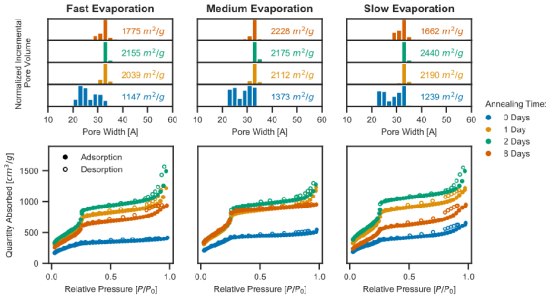

N_2 gas-sorption isotherms (above) show that films made directly from monomers initially have a wide distribution of pore sizes and low surface area regardless of the evaporation rate. However, if the films were annealed in ethanol in the presence of residual TFA, after two days very high surface areas and narrow pore size distributions could be achieved.

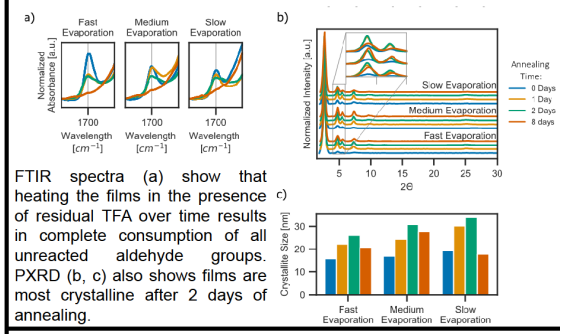

FTIR spectra (a) show that heating the films in the presence of residual TFA over time results in complete consumption of all unreacted aldehyde groups. PXRD (b, c) also shows films are most crystalline after 2 days of annealing.

Summary: A facile, scalable process for casting free-standing, imine-based 2D polymer films tens of microns in thickness directly from a solution of monomers in TFA and water has been developed. Highly-crystalline films with surface areas (2,200–2,400 m2/g) approaching the theoretical maximum could be achieved by controlling the initial film formation conditions and by heating the produced films in ethanol with a small amount of residual acid.

Engineering III-Nitride Semiconductor Materials for Solar-Driven Chemical Energy

Vijay S. Parameshwaran
U.S. Army Research Laboratory, Sensors and Electron Devices Directorate, Adelphi, MD 20783

Introduction & Motivation

- **Solar-driven chemical reactions:**
  - Water to hydrogen gas

$$H_2O + h\nu \rightarrow \frac{1}{2}O_2 + H_2$$

  - Carbon dioxide to high-order fuels

$$CO_2 + 2H_2O + h\nu \rightarrow \frac{3}{2}O_2 + CH_3OH$$

Onsite fuel generation for army deployment

- **Electrical junction studies of nanomaterials**
  - Liquid Schottky barrier at interface
  - Direct analog to solar fuels reactions
  - Testbed for materials, electronic, and photonic properties with scaling

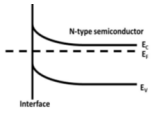

- **Why III-Nitride Semiconductors?**
  - Direct bandgap tunability for light absorption and photovoltage
  - High crystallinity for charge transport and low SRH recombination
  - Inherent chemical stability, and with engineering passivation layers

Structured GaN

- **Control of film, microwires, and nanowires**
  - *Change film (and junction) with source material amount and spacing using reactive vapor phase transport*

Thick Films | Mixed Films/Wires | Nanowires w/ Islands

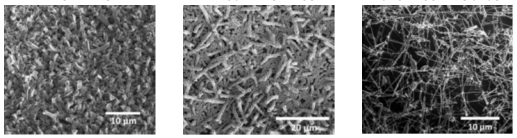

- *Films are polycrystalline, nanowires and islands are single crystal*

•Photoanode configuration on p⁺ silicon

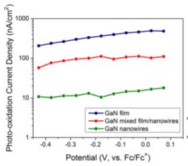

- *Ferrocene oxidation shows photocurrent from only GaN; trend with material volume*
- *Impedance spectroscopy with cobaltocene shows different junction electrostatics with morphology, reflected in band diagrams*

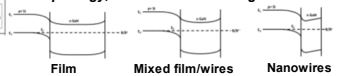

J. Electrochem. Soc. 163 (10), pg. H958-H963, 2016

InN Nanowires

- **Control of wire shape through VLS growth process**
  - *In-catalyzed with thermal gradient: "ice cream cone" structure*
  - *Au-catalyzed at low temperature: wide-base faceted cone*

Indium Catalyzed | Gold Catalyzed

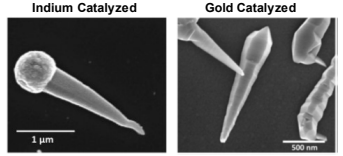

- *Both nanowire forms are wurtzite hexagonal binary InN, and single crystal*

•Photoanode configuration on p⁺ silicon, cobaltocene

- *Cobaltocene oxidation under solar flux shows photovoltage, but capacitance shows highly charged interface consistent with InN surface accumulation*

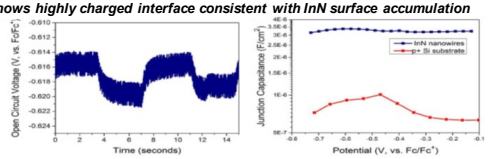

ACS Appl. Mater. Interfaces, 8 (33), pg. 21454-21464, 2016

Polarization Control of c-plane InGaN

- *III-Nitride semiconductors have a piezoelectric polarization field in the c-plane direction from cation/anion diplole; controls electrostatics and carrier dynamics*

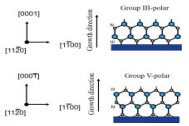

Nonpolar | III-Polar | V-Polar

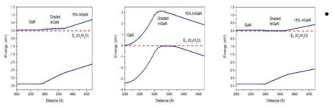

- *InGaN photoanode electrostatics fundamentally different based on polarization*
- *Epitaxial III-Polar InGaN shows reduced photocurrent despite larger spectral range; consistent with drift-diffusion modeling of the material*

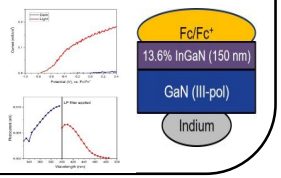

ECS Fall Meeting, 2017

III-Nitride MBE on Silicon

GaN Nanowire Arrays

InN Microcrystals

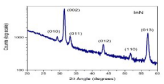

Epitaxial GaN and InGaN Films

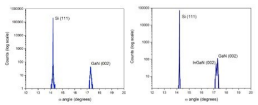

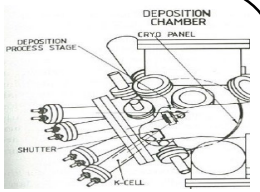

- *Use thermodynamic and kinetic control with molecular beam epitaxy (MBE) to grow heterojunctions, microcrystals, and nanowires on silicon*
- *Template for designing photoelectrode materials (anode and cathode) for hydrogen generation and CO_2 reduction*

Cu-based Catalyst Synthesis

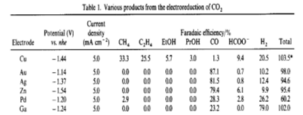

- *Copper is unique among metals in the products it can make from CO_2 reduction catalysis (alcohols, methane)*
- *MBE explored as a technique to synthesize copper-based catalysts in vacuum-preserved interface for: fundamental studies, integration on light absorbers, and on carbon supports for reactor designs*
- *Tuning can be achieved with surface crystal orientation and indium/gallium alloying*

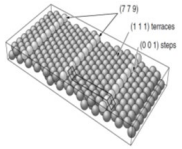

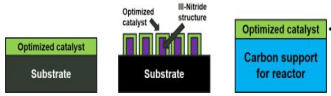

- *Electrode designs can be adjusted for III-Nitride surfaces, nano and microstructures, and reactor assemblies*

TECHNOLOGY DRIVEN. WARFIGHTER FOCUSED.

Determining the Solvation Structure of Aqueous Aluminum Electrolyte

Glenn Pastel,[*a] Ying Chen ,[*b] Alan Zheng ,[*c] Marshall Schroeder,[a] Travis Pollard, [a] Michael Ding,[a] Oleg Borodin, [a] Steven Greenbaum, [c] Karl Mueller, [b] Kyle Grew,[a] and Kang Xu[a]
office: Bldg 207 Z2A -05-17 email: glenn.r.pastel.civ@army.mil
[a]Battery Sciences Branch, SEDD Division, Army Research Laboratory, Adelphi, MD, 20873, USA

Motivation

Aqueous Al batteries boast impressive metrics including: (i) ***higher energy density than Li-ion batteries (> 450 Wh kg^{-1})***, (ii) ***inflammability***, and (iii) ***low raw material cost***, however solvation and species activity are not well understood.

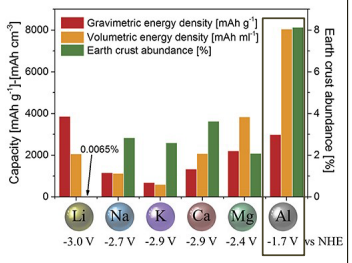

Leisegang, et al. *Front Chem.* (2019)

Solvation Structure

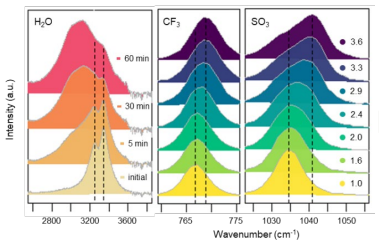

Gas Evolution

Electrolyte: 1m Al(Tf)$_3$-H_2O

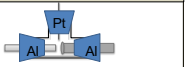

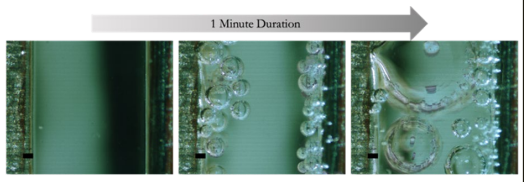

Thermodynamics

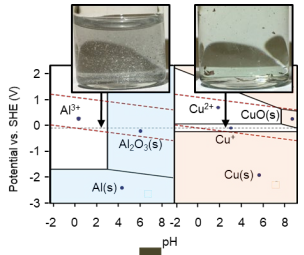

Dehydration

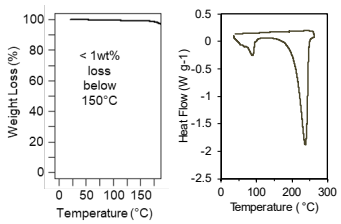

Transport Properties

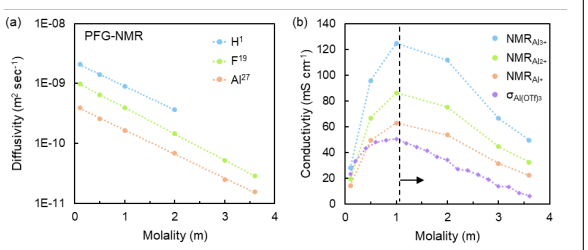

In collaboration with Prof. Greenbaum, Hunter College

Electrochemical Performance

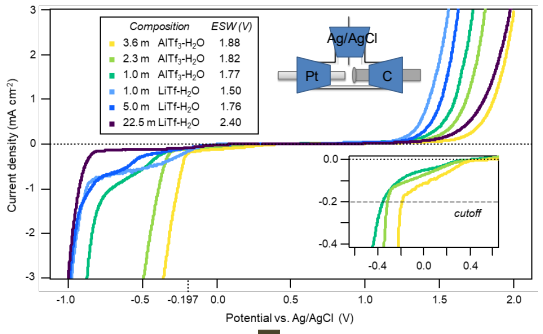

Conclusions

(1) We found compelling evidence for partial hydrolysis and shielding of OH^- in the first solvation shell of Al^{3+} with limited CIP formation.
(2) This work clearly delineates the differences between classic water in-salt electrolytes and the Al(OTf)$_3$-H_2O system.
(3) High proton activity will limit the outlook of future aqueous aluminum batteries for the Soldier.

Manuscript under preparation for submission to *Energy & Environmental Science*
In collaboration with [b]Pacific Northwest Nation Laboratories & [c]Hunter College, CUNY

Communication-Efficient Device Scheduling for Federated Learning Using Stochastic Optimization

J. Perazzone[1], S. Wang[2], M. Ji[3], K. Chan[1]
Email: jake.b.Perazzone.civ@army.mil

[1]Army Research Laboratory, FCDD-RLC-NT, Adelphi, MD , 20783, USA
[2]IBM Thomas J. Watson Research Center, Yorktown Heights, NY 10598, USA
[3]Electrical and Computer Engineering Department, University of Utah, Salt Lake City, UT 84112, USA

Background and Motivation

Federated Learning (FedAvg Algorithm)

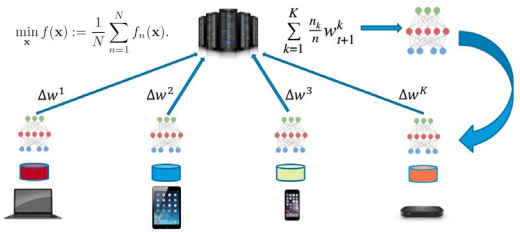

What is federated learning?

- It is a distributed machine learning framework where users contribute to a shared model, but data remains on users' devices

Benefits
- User Data Privacy
- "Communication-efficiency"

Challenges
- Data and system heterogeneity
- Communication bottleneck

Problem Statement

How can we optimally choose clients each round in order to minimize the communication costs, but still ensure convergence? Especially in tactical networks where resources are constrained and connectivity can be intermittent.

Our Approach:
- Derive convergence bound for non-convex functions with arbitrary selection probabilities for each client each round
- Design optimization problem that minimizes a function of the derived convergence bound and the time spent communicating the parameters
  - Variables: selection probabilities, transmit power
  - Constraints: max transmit power, average transmit power

Army Relevance
- This technology can be used to more rapidly learn and refine the ML models that are currently deployed in the field to increase performance metrics such as classification accuracy and prediction error without expensive data transfer. Possible use-case: spectrum sensing.

Communication model
- Wireless
- Assume TDMA
- Independent Rayleigh fading with parameter σ_i^2

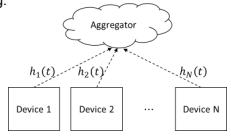

Optimization Problem

Minimum time required to transmit model
ℓ: size of model (bits)
B: bandwidth
$h_n(t)$: channel gain
$P_n(t)$: transmit power
N_0: noise power

From convergence bound

Prioritization parameter

$$\min_{\{q_n^t\},\{P_n(t)\}} \lim_{T\to\infty}\frac{1}{T}\sum_{t=0}^{T-1}\mathbb{E}\left[\sum_{n=1}^{N}\left(\frac{1}{Nq_n^t}+\lambda\frac{\ell q_n^t}{B\log_2\left(1+|h_n(t)|^2\frac{P_n(t)}{N_0}\right)}\right)\right]$$

$$\text{s.t.}\quad \lim_{T\to\infty}\frac{1}{T}\sum_{t=0}^{T-1}\mathbb{E}\left[P_n(t)q_n^t\right]\le \bar{P}_n,\ \forall n=1,\dots,N$$

$$0\le P_n(t)\le P_{\max},\ n=1,\dots,N$$

$$q_n^t\in(0,1]$$

Time average power constraint

Lyapunov Drift-Plus-Penalty Framework

$$\min_{\{q_n^t\},\{P_n(t)\}} f(q_n^t,P_n(t)) := Vy_0(t)+\sum_{n=1}^{N}Z_n(t)y_n(t)$$

$$\text{s.t.}\quad 0\le P_n(t)\le P_{\max},\quad \forall n=1,\dots,N$$

$$q_n^t\in(0,1].$$

$$Z_n(t+1)=\max[Z_n(t)+y_n(t),0],\qquad y_n(t)=P_n(t)q_n^t-\bar{P}_n.$$

Client Scheduling Policy

- **Optimization problem solution:**
  - Solve above each round
  - Optimization is independent for each n, so we can solve for each $q_n^t, P_n(t)$ separately
  - We obtain an analytical solution

Algorithm 2: Stochastic client sampling

Input: $h_n(t)$, N_0, ℓ, B, V, λ, $P_{\max}$, $\bar{P}_n$
Output: q_n^t, $P_n(t)$

$Z_n(0)\leftarrow 0$;
$P_n(0)\leftarrow P_{\max}$;
$q_n^0\leftarrow \min\{\max\{\sqrt{\frac{B\log_2\left(1+|h_n(t)|^2\frac{P_{\max}}{N_0}\right)}{N\lambda\ell}},0\},1\}$;
for $t\leftarrow 1,\dots,T-1$ **do**
  for $n\leftarrow 1,\dots,N$ *in parallel* **do**
    Calculate roots via (16) and (17);
    if $0\le P_n(t)\le P_{\max}$ *and* $q_n^t\in(0,1]$ **then**
      Perform Hessian determinant test to ensure minimum
    else
      $P_n(t)\leftarrow P_{\max}$
      $q_n^t\leftarrow \min\{(17),1\}$
    $Z_n(t+1)\leftarrow \max[Z_n(t)+P_n(t)q_n^t-\bar{P}_n,0]$

Conclusions

By intelligently selecting users, we can converge to a good model in less time (compared to standard uniform selection) thus using less network resources without direct knowledge of the channel statistics.

Results

Homogeneous Channel Gain
- All nodes have Rayleigh fading with parameter $\sigma = 1$

Heterogeneous Channel
- 10 clients have $\sigma = 0.2$
- 40 clients have $\sigma = 0.75$
- 50 clients have $\sigma = 1.2$

Notes
- Homogeneous channel case
- Our algorithm first reaches an accuracy of 0.7 in 79.2% less time
- Heterogeneous channel case
- Our algorithm first reaches an accuracy of 0.7 in 58.2% less time

CIFAR-10 Dataset

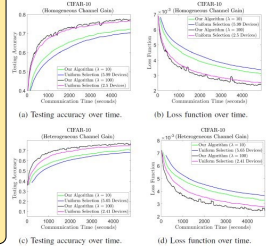

(a) Testing accuracy over time. (b) Loss function over time. (c) Testing accuracy over time. (d) Loss function over time.

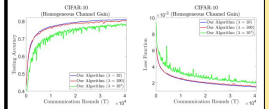

(a) Testing accuracy over rounds. (b) Loss function over rounds.

Fig. 3: Effect of λ (CIFAR-10).

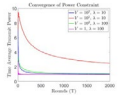

Effect of λ
- Prioritizes minimizing comms instead of converging
- Converges more slowly per iteration, but can perform more iterations per second
- Very large λ results in very low selection probabilities

Effect of V
- Traditionally controls trade-off between average queue length and distance from optimal objective
- No real queues: controls trade-off between convergence of satisfying constraint and distance from optimal objective

Heterogeneous Channel
- 500 clients have $\sigma = 0.2$
- 1500 clients have $\sigma = 0.75$
- 1597 clients have $\sigma = 1.2$

Notes
- The percentage of speed up is better for the $\lambda = 10$ case than the $\lambda = 100$ case.
- Testing accuracy reaches 0.8 in 69.5% less time in the $\lambda = 10$ case compared to its uniform 86.2% less time in the $\lambda = 100$ case compared uniform equivalent.

FEMNIST Dataset

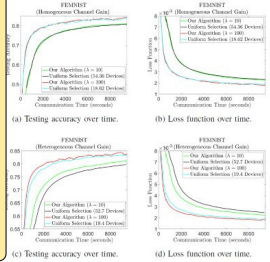

(a) Testing accuracy over time. (b) Loss function over time. (c) Testing accuracy over time. (d) Loss function over time.

J. Perazzone, S. Wang, M. Ji, and K. Chan "Communication-Efficient Device Scheduling for Federated Learning Using Stochastic Optimization," *submitted*. 2021

BOLD activity variability as a neural marker of fatigue on sustained alertness tasks

Italo'Ivo Pinto[1], Kanika Bansal[1,2], & Javier Garcia[1]

[1] US CCDC Army Research Laboratory, Aberdeen Proving Ground, MD

[2] Department of Biomedical Engineering, Columbia University, New York, NY

Motivation

The advances on sensor technologies and widespread use of technological gadgets will turn the future battlefield into a dynamical and stimulus rich environment such that the ability to maintain attention and respond rapidly will be crucial to overcome the information overload and deploy a fast response to various demands. In this context, the ability to maintain alertness and attention for a sustained amount of time is essential for a wide range of tasks, and has severe consequences on other aspects of cognition and decision making.

In this work we explore the neural markers that correlate with performance in an attention demanding task, and how it is affected for sustained attention demand during the task.

Experiment design

- The experiment was designed to capture longitudinal data with naturalistic sleep patterns.
- The data was collected in 8 biweekly sessions, with 58 subjects.
- The study investigated 5 tasks with different cognitive demands: Psychomotor vigilance, dot probe, modular math, visual working memory, and dynamical attention.
  - The psychomotor vigilance test (PVT) is used to measure alertness and reaction time.
  - Result of PVT can be substantially affected by sleep deficits and fatigue [1].

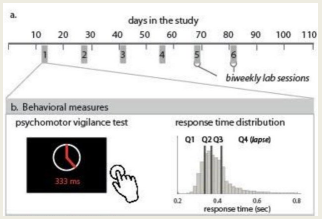

Methods

The blood-oxygen-level-dependent (BOLD) activity variance was used to explore the relation of putative input and output networks activity dynamics.

- The activity variance indicates how abrupt are the changes on activity amplitude, being a measure of neuronal activity speed [3].
- The ratio of the activity variance between two regions/ networks indicates how balanced are the neuronal activity speed between them.
- Here, we looked at this ratio for Visual (input) and Somatomotor (output) networks to assess the neuronal activity speed balance.

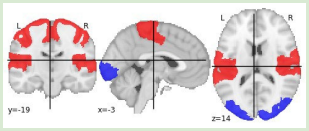

O/I variance ratio < 1 → faster activity in the input.

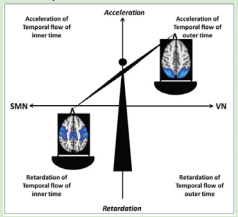

O/I variance ratio = 1 → balance of the activity between the two networks.

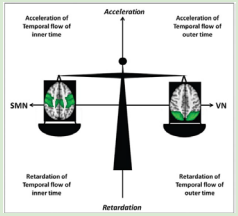

O/I variance ratio > 1 → faster activity in the output.

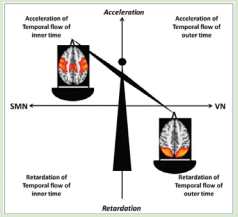

Is this perception of time speed associated with behavior and performance on tasks?

Results

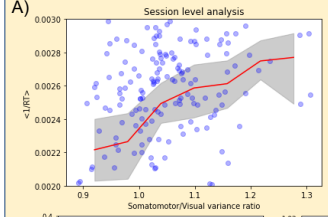

- We used (1/RT) as a measure of task performance on PVT.
- In a session level analysis we can observe that the mean of the performance score increases as the ratio of the variability of activity in Visual and Somatomotor networks increases.

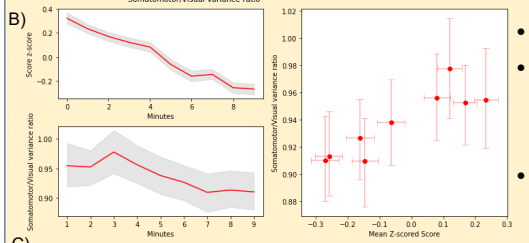

- In general, PVT performance degrades along the task [1].
- Investigation of the task scores and the Visual/Somatomotor activity variance calculated every minute along the task shows that the two measures are correlated.
- Here we hypothesize that the fatigue accumulation during the task drives this effect.

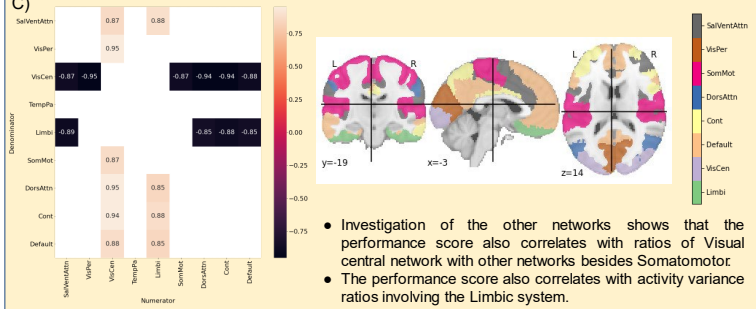

- Investigation of the other networks shows that the performance score also correlates with ratios of Visual central network with other networks besides Somatomotor.
- The performance score also correlates with activity variance ratios involving the Limbic system.

Conclusions and future directions

- The O/I variance ratio correlates with task performance, when visual central and limbic networks are used as inputs.
- We are further analyzing pupil dynamics during PVT to assess how arousal and pupil dilation relate with the O/I variance ratios.
- Investigation of how activity speed balance influences other tasks is also currently ongoing.

Bibliography

[1] Basner, M., & Dinges, D. F. (2011). Maximizing sensitivity of the psychomotor vigilance test (PVT) to sleep loss. *Sleep*, *34*(5), 581-591.

[2] Schaefer A, Kong R, Gordon EM, Laumann TO, Zuo XN, Holmes AJ, Eickhoff SB, Yeo BTT. Local-Global parcellation of the human cerebral cortex from intrinsic functional connectivity MRI. Cerebral Cortex, 29:3095 -3114, 2018

[3] Northoff, G., Magioncalda, P., Martino, M., Lee, H. -C., Tseng, Y. -C., & Lane, T. (2018). Too Fast or Too Slow? Time and Neur onal Variability in Bipolar Disorder —A Combined Theoretical and Empirical Investigation. Schizophrenia Bulletin, 44(1), 54 –64. https://doi.org/10.1093/schbul/sbx050

Flexible coding of adaptive decision choices in humans and artificial neural networks

Nuttida Rungratsameetaweemana[1,2], Kanika Bansal[1,3], Javier O. Garcia[1]

[1]U.S. CCDC Army Research Laboratory, Aberdeen Proving Ground, MD; [2]The Salk Institute for Biological Studies, La Jolla, CA; [3]Department of Biomedical Engineering, Columbia University, New York, NY

Abstract

The brain contains billions of neurons, each connecting with up to 10,000 others. Together, these neurons continually produce electrical signals to represent information about the sensory environments. A fundamental question in neuroscience and artificial intelligence concerns how adaptive decisions can be consistently and flexibly generated given the spatiotemporal complexities of naturalistic sensory information. The present study addresses this question through a complementary blend of human psychophysics, electroencephalography (EEG), and artificial neural networks.

Experimental task paradigm

Assessing behavioral and neural dynamics of flexible decision making

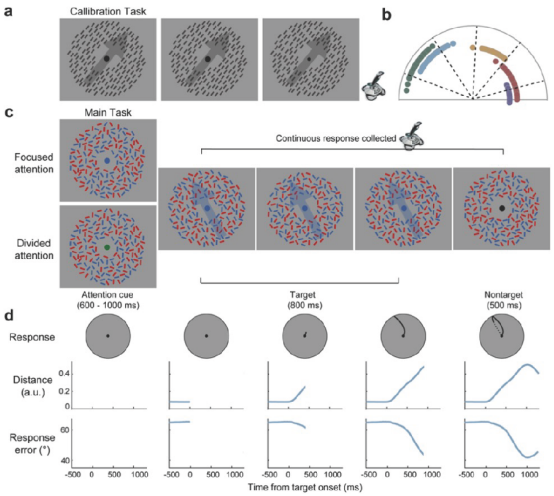

Acknowledgement

We are grateful for invaluable feedback and discussion from Drs. Robert Kim, Terrence Sejnowski, and John Serences

Recurrent neural network (RNN) model

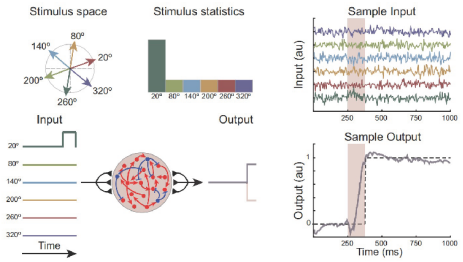

$$\tau \frac{dx}{dt} = -\boldsymbol{x}(t) + \boldsymbol{w}\boldsymbol{r}(t) + \boldsymbol{w}_{in}\boldsymbol{u}(t) + \xi$$

$$\boldsymbol{r}(t) = \sigma(\boldsymbol{x}(t)) = \frac{1}{1+\exp(-\boldsymbol{x}(t))}$$

$$\boldsymbol{o}(t) = \boldsymbol{w}_{out}\boldsymbol{r}(t) + b$$

- τ: synaptic time-constant
- $\boldsymbol{x} \subset \mathbb{R}^{N\times T}$: synaptic current variable
- $\boldsymbol{r} \in \mathbb{R}^{N\times T}$: neural firing rate
- $\boldsymbol{u} \in \mathbb{R}^{N_u\times T}$: time-varying input
- $\boldsymbol{o} \in \mathbb{R}^{1\times T}$: neural population activity

RNN behavioral performance

Both humans and RNNs use top-down control to optimize decisions

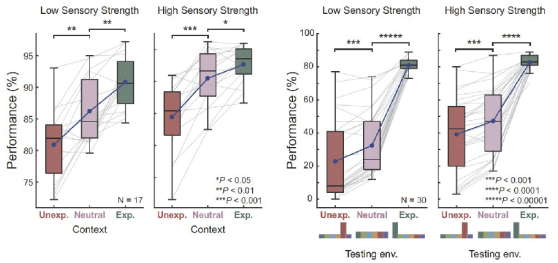

Conclusions

- Biologically realistic RNNs dynamically incorporate top-down knowledge into their decisions in the same manner as humans.
- By dissecting the trained RNNs, we demonstrate how competitive inhibition and recurrent excitation form the basis for neural circuitry important for adaptive decision making.

Temporal dynamics of human behavior

Dissociable effects of top-down control on decision making

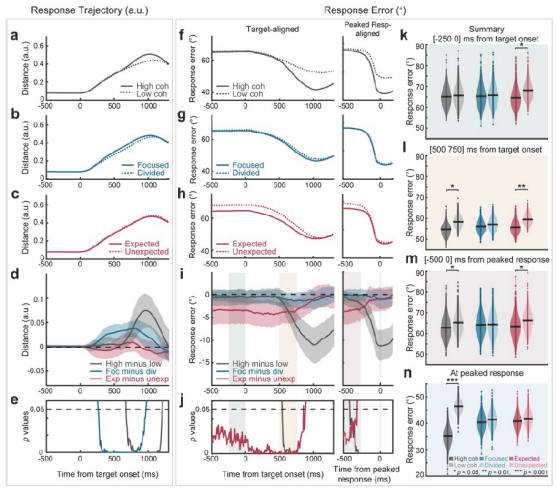

Mechanisms for flexible coding of decision choices

Decreased within-group inhibition and increased within-group excitation of the neural subgroup selective for most likely stimulus

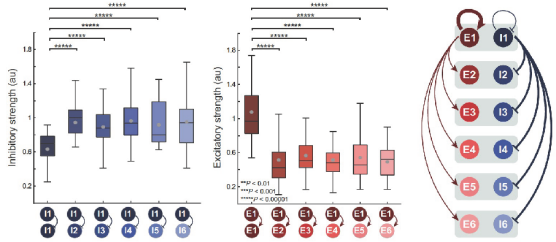

Data-Driven Chemical Kinetic Reaction Mechanism for F-24 Jet Fuel

POC: Je Ir Ryu (j.ryu@anl.gov)
Advisor: Chol-bum "Mike" Kweon

VICTOR ERP

Versatile TaCTical pOwer and pRopulsion (VICTOR) ERP
- Multi-Fuel Capable Hybrid Electric Propulsion (MCHEP)

- Uncontrolled fuel properties
- Logistics burden
- Extreme operating conditions

MQ-1C Gray Eagle Unmanned Aircraft System | Thielert Centurion 1.7 Heavy-Fuel Engine | Mercedes-Benz A 170 CDI

Objectives

Develop jet fuel chemical kinetic mechanism at the Army-relevant operating conditions

- Accuracy at intermediate and low temperature regions (750 to 850K)
- Based on conventional mechanism platform
- Use a ML/AI method for optimization

Past: JP-8
Current: Jet A (commercial fuel)+3 military additives

Challenges

Low Temperature Oxidation Chemistry

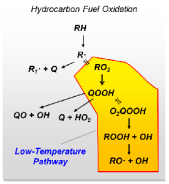

- Complicated sequence of reactions
- Multi-stage ignition behavior
- Requires a good understanding of reaction pathways

→ Not feasible!

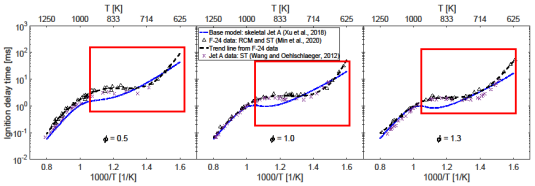

Approach

Chemical kinetic model CHEMKIN format

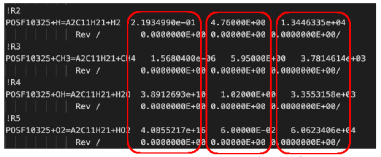

$$k = AT^{b}\exp\left(-\frac{E_a}{RT}\right)$$

Genetic Algorithm

Data-driven Mechanism: Genetic Algorithm

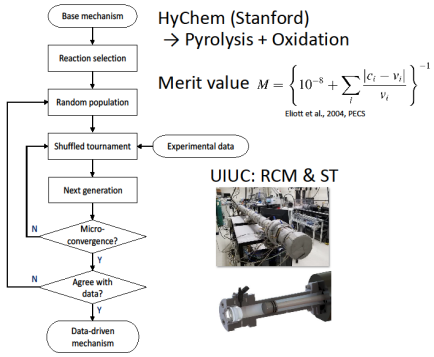

HyChem (Stanford)
→ Pyrolysis + Oxidation

Merit value $M = \left\{10^{-8} + \sum_i \frac{|c_i - y_i|}{y_i}\right\}^{-1}$

Elliott et al., 2004, PECS

UIUC: RCM & ST

Initial Trial

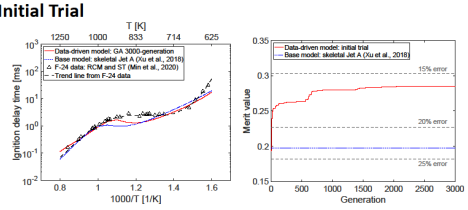

Results & Discussion

Development Techniques

- Numbers of population and modified reactions
- 2-stage sets / manual selection

ARLMech-HC-F24

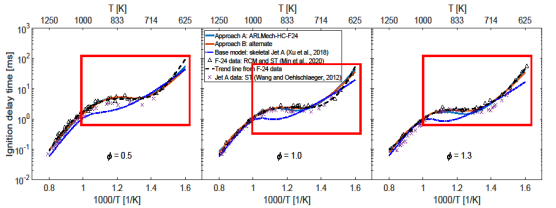

		Approach A: ARLMech-HC-F24
Parameters	Number of data points	51 (ϕ = 0.5, 1.0, 1.3)
	Number of modified reactions	16
	Population size	52 + 1
Techniques	Data distribution	Evenly-spaced
	Selection of reactions	Manual set: pyrolysis and NTC submodels
	Optimization variables	A, E_a

- ARLMech-HC-F-24 is developed that predicts ignition behavior accurately in intermediate/ low temperature regions
  - B may include non-physical behavior
  - A (ARLMech) is suggested

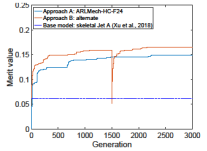

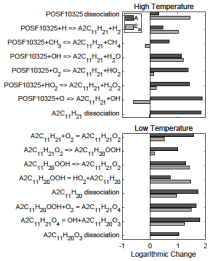

Path Forward

New fuels: ARLMech-HC-ATJ, ARLMech-HC-F24/ATJ

Applications and collaborations

RCM experiment/simulation: UIUC/ANL

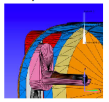

Engine simulation: UW

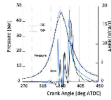

High-fidelity CFD: SNL

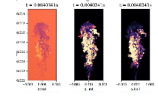

M1 gas turbine ignition/combustion: ANL/ARL

Mechanism optimization using ActivO: ANL

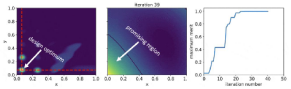

Apparatus and Techniques for the Deployment and Characterization of Event-based Sensors in Protection Systems

Jonah Sengupta

JOHNS HOPKINS WHITING SCHOOL of ENGINEERING

Abstract

Event-based cameras offer a size and weight efficient sensing platform that does not emit a signature but can be used in active protection applications. Despite the promise of event-based cameras, little progress has been made to mature the technology in realm of protection. Current sensing modalities, such as radar and LIDAR, have been equipped with infrastructure to allow expedient testing in range scenarios and vetted to understand the limitations of each technology with reference to threat velocity profiles. a series of equipment, test fixtures, and techniques that have been recently developed to characterize and deploy event-based sensors in APS scenarios. Initial experiments have been done to characterize scene velocities, communication latencies, and hardware capabilities. **Camera collection interactions under 50us have been seen, rotational velocities of 200rpm are detected, and a complete profile of delays was acquired.**

Objectives

- Design and implementation of motor-mount stand for velocity characterization
- Design and deployment of embedded communication device for event-based sensors

Materials and Methods

Event-Based Sensor

DAVIS 346 and Tele Lens

Specification	Value
Spatial Resolution	346x240
Temporal Resolution	1us
Max Throughput	12 million events per second
Dynamic Range	120 dB
Dimensions	40x60x25mm
Weight	100g
Power consumption	0.9W

Sensor Specifications

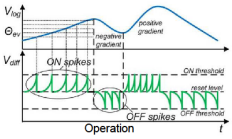

Operation

- Inspire by the mammalian retina, event-based sensors ***asynchronously*** respond to ***changes in intensity*** rather than encode absolute values in frames
- Positive changes produce **ON** events and negative changes produce **OFF** events

Motor-mount for Optical Stimuli

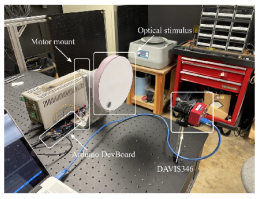

- Optical stimulus attached to stepper-motor produces a moving pattern for event camera rotational velocity characterization
- Stepper motor can spin at max speed of 400 rpm – speeds are programmed by Arduino board
- Aluminum motor mount was designed to be compatible with 1" optical table

PiBox: event-based experiment platform

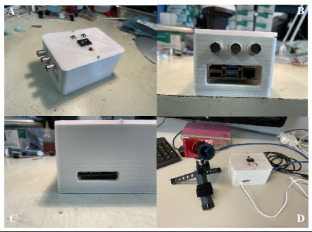

- Raspberry Pi-based platform to attach hardware triggering and communication interfaces to event-based sensing frontend
- Integrated level shifters interface Pi GPIO to TTL signaling used for range testing
- Switches, button, and LEDs are used for diagnostics

Results

Stereo Rotational Velocity Capture

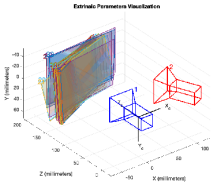

Calibration pattern for stereo

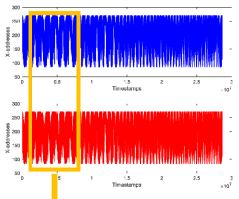

Extracted velocity from stereo capture:
5 distinct levels from 50 to 200 rpm

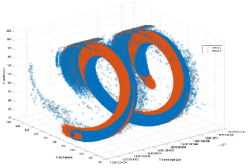

Stereo capture of rotating dot:
orange is left cam, blue is right

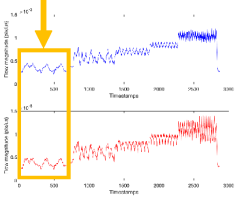

PiBox Latency Characterization

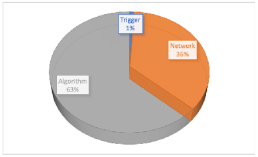

Latency contribution: algorithm consumes large amount of time and has large jitter

	Trigger	Network	Algorithm	Total
Mean	18.53	663.67	1181.82	1864.012
Standard Deviation	4.06	95.25	1036.22	1135.53
σ/μ	0.22	0.14	0.88	--

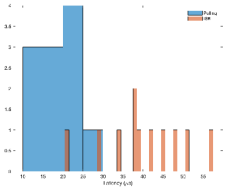

Latency histograms from PiBox:
Blue – polling scheme, Orange - interrupts

Conclusions

- Rotational velocities ranging from 50 to 200 rpm were detected using the motor mount set-up
- Latencies of less than 50us using hardware triggers were used to collect camera data
- Algorithm optimization and localization of processing is needed

Future Steps

- **Use optical data for depth:** using the given stereo setup, depth resolution can be characterized
- **Improve PiBox**: hardware and box construction can be improved to allow for increased trigger capabilities and range hardiness.

Acknowledgements

- This work and effort has been sponsored by the DoD-funded SMART Fellowship
- The author would like to thank Aaron Bard for his support in construction of testing equipment

Production of Core-Shell Aluminum Nanoparticles via Scalable Atmospheric Plasma Surface Treatment and Coating

Dinesh Thapa[1], Rose A. Pesce-Rodriguez[1], Lily Giri[1], and Scott D. Walck[2], Chi-Chin Wu[1]
Email: dinesh.thapa.ctr@army.mil; 1: FCDD-RLW-WA, 2: FCDD-RLW-MC

Background

Core-shell aluminum nanoparticles (nAl) are of great interest due to their high heat of combustion and rapid energy release rate. However, the presence of an intrinsic passivating oxide layer often inhibits their performance. In the proof of demonstration, previous studies have shown the feasibility of making reactive nAl with thinned oxide shell after atmospheric pressure plasma surface treatment and coating using carbon monoxide as the precursor in custom-made dielectric barrier discharge (DBD) plasma reactors. Key plasma experimental conditions were identified from preliminary efforts with capabilities of producing energetic carbon-coated nAl (nAl@C) with ~200 mg yield per batch. **Ongoing scale-up efforts have been conducted to produce samples in a large batch ~500 mg using a larger DBD reactor.**

Objective

- Explore the viability of scalable atmospheric plasma surface treatment to produce large bath quantities of plasma-treated nAl.
- Perform in-depth characterization of 500 mg batch-size plasma treated nAl and compared with the small batch of the nAl produced in a small reactor.

Acknowledgment

This work is supported by the US Department of Defense, Office of the Under Secretary for Defense for Research and Engineering, Applied Research for the Advancement of S&T Priorities Program on Enhanced Energetic Effects

Reference:

Wu *et al.* J. Appl. Phys.,**129**:063301 (2021)

Experimental set up

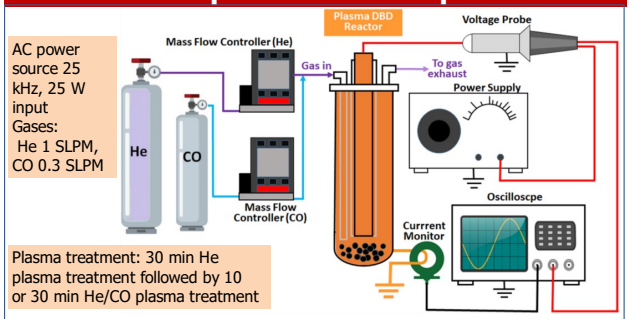

Schematic view of experimental set up; ref (1)

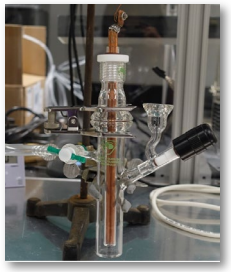

1" reactor, 200 mg per batch
Previous study

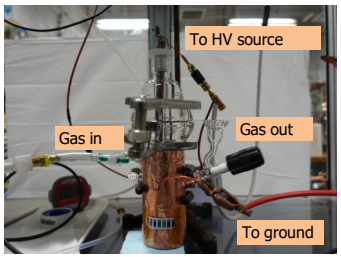

2" reactor, 500 mg per batch,
current study

He plasma-treated nAl: TEM

He Plasma-treated nAl utilizing a large reactor exhibits features with the consistent results in the previous study for small scale.

- Distinct intact Al core
- Thinned oxide shell thickness of ~ 2-3 nm relative to ~5-6 nm in as-received nAl.
- Sporadic deposits of γ-Al_2O_3 phase on the surface of nAl.

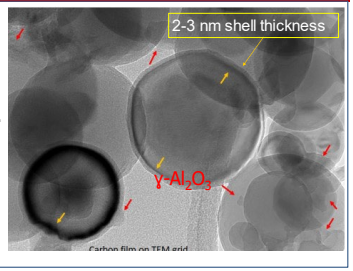

Elemental mapping: nAl@C

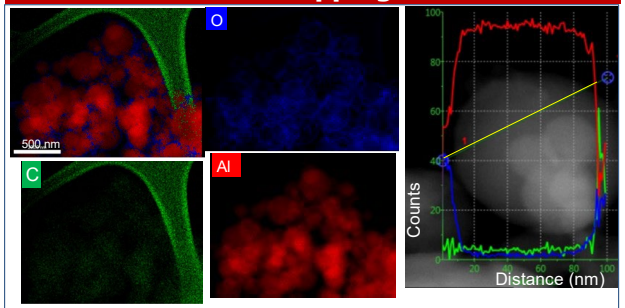

Elemental mapping in scanning TEM mode (STEM) of 30 min HE/CO plasma-coated Al@C sample: The maps (clockwise from the top left) are overlaid of all elements, Oxygen (O, blue), aluminum (Al, red), carbon(C, green). O outlined the spherical shapes of the particles with local concentration at γ-Al_2O3 deposits. C showed the uniform dispersed nature of the Gcoating on Al@C surface.

High-angle annular dark-field image of a single particle in STEM mode displaying the count profile for each element Al, C and O corresponding to the yellow line.

Surface chemical analysis: FTIR

Peaks between 1700 and 1100 cm^{-1} in the plasma He/CO-treated nAl indicates the formation of Aluminum carboxylate as small batch samples. The peaks appeared to be prominent for 30 min He/CO.

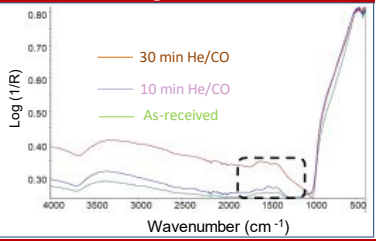

Conclusions and path forward

- Plasma-treated nAl utilizing the large 2" reactor resulted a relatively large batch yield with properties including thin oxide shell, preserved active Al core, and uniformly distributed carbonaceous coating similar to the findings reported for the nAl produced in the small reactor with high energetic performance.
- Efforts will be made on enabling plasma diagnostics capabilities and in-processing real time measurements
- The influence of various experimental variables will be further investigated.

Determining Phase Coexistence Curves for Fully Atomistic Models of RDX and HMX

Garrett M. Tow, James P. Larentzos, John K. Brennan (*FCDD-RLW-WA*)

Problem: 1st Order Phase Transitions

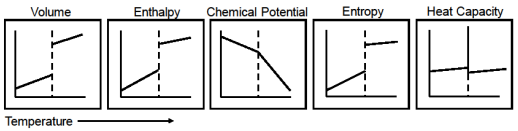

Solution: PseudoSuperCritical Path (PSCP)

Avoid 1st order phase transitions by thermodynamically integrating between hypothetical intermediate states that smooth the phase transition

$$\Delta A = \int \left\langle \frac{\partial U}{\partial \lambda} \right\rangle_{\lambda} d\lambda$$

$$\Delta G = \Delta A + \int_{V_1}^{V_2} \langle P \rangle dV$$

Gibbs–Helmholtz Integration

$$\Delta G_{2,l\to s} = T_2 \left(\frac{\Delta G_{1,l\to s}}{T_1} - \int_{T_1}^{T_2} \frac{\Delta \langle H \rangle_{NPT,l\to s}}{T^2} dT \right)$$

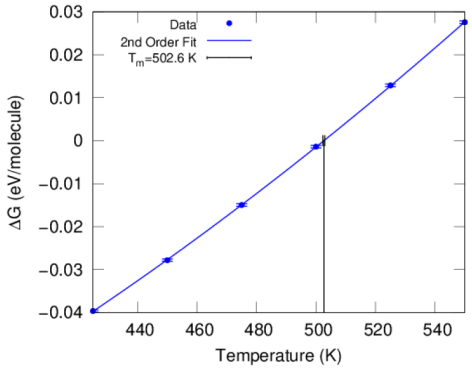

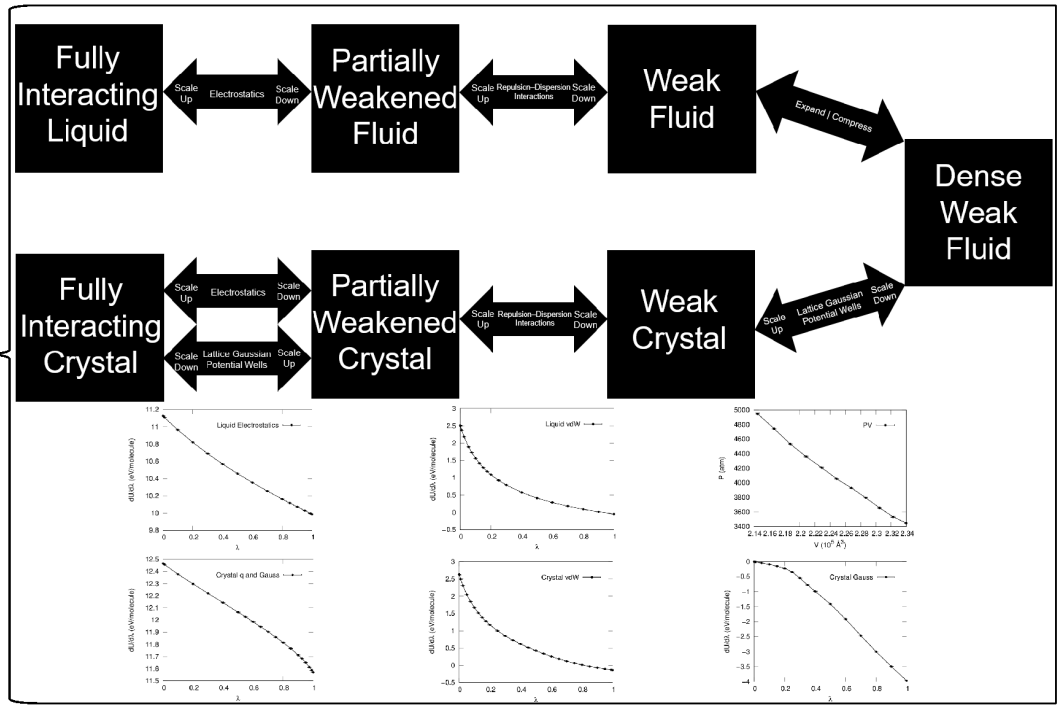

α-RDX Melt

β-HMX Melt

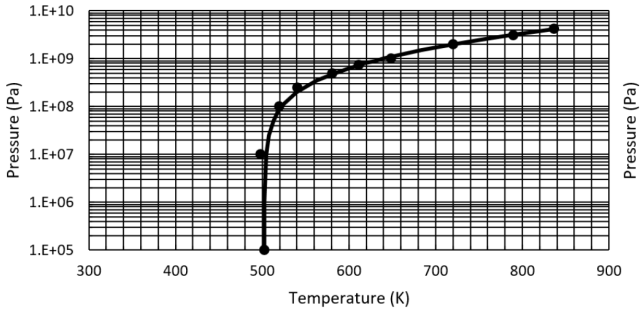

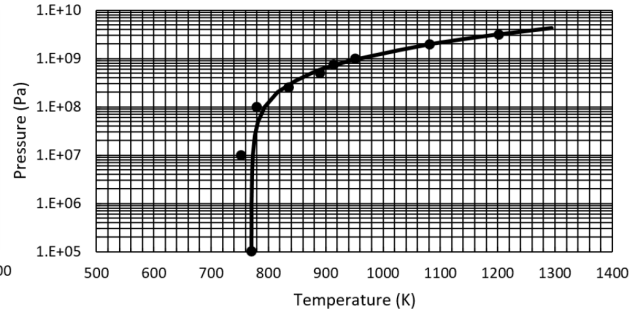

DESIGNING EFFECTIVE PROBLEM-SOLVING TEAMS USING AGENT-BASED MODELING

Malgorzata Turalska[1], Rosie Lickorish[2], Geeth De Mel[2], Hugo McNally[3], Sebastian Stein[4]

[1] Network Science Division, CSID, CCDC ARL; [2] IBM Research Europe, UK; [3] Imperial College, UK; [4] University of Southampton, UK

Problem statement and motivation

Teamwork lies at the cornerstone of the modern workplace, allowing organizations to tackle problems whose complexity reaches beyond the abilities of individuals. Similarly, the complexity of modern military operations creates a demand for efficient collaborative decision making and problem solving. Since an effective operability in dynamic environments requires precise dissemination and transfer of information across the command-and-control structure, the key question remains what types of social interactions are most suitable for achieving necessary C2 capabilities.

What is the optimal configuration of a group to produce the best possible collective output ?

Learning strategy strongly affects the success of collective search

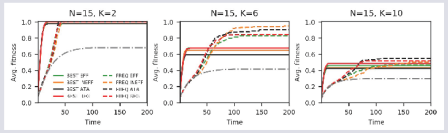

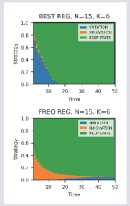

Teams that prefer imitation (BEST) of other agents in the social network reach collective solutions faster than teams performing more individual exploration (FREQ), however, that comes at a cost of lower performance in highly complex landscapes. Moreover, the latter learning strategy leads to improved collective outcomes in landscapes of intermediate complexity.

Differences in social network structure have little effect on the search process, however, performing a collective search is always better than searching alone (grey line). Additionally, comparable performance is achieved by densely and sparsely connected teams of the same size, indicating that high connectivity is not necessary for efficient teamwork.

Intermittent social learning improves collective problem solving

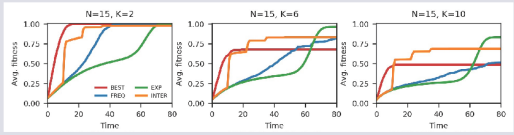

The incorporation of a temporal component into the learning strategy results in comparable or better outcomes than ones obtained in the case of static policies. The EXP rule of executing an extensive individual search followed by social learning operates similarly to the FREQ strategy, however, due to the longer period of individual learning and stronger presence of imitation, it outperforms the latter case. Furthermore, the intermittent strategy (INTER) is also an improvement over BEST and FREQ rules, since it results in outcomes equal or better than the FREQ rule but achieves them in a much shorter time.

Altogether our results indicate that pattern of team interactions is the most important factor in improving group performance, where frequent communication works well for simple problems. In the case of complex problems, infrequent group interaction and a high level of autonomy are necessary to achieve the best results.

Reinforcement learning generates effective learning policies

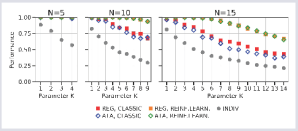

Finally, we investigate the utility of reinforcement learning (RL) in establishing efficient teamwork protocols. We demonstrate that the Q-learning algorithm outperforms outcomes of agent-based modelling for intermediate and highly complex tasks, suggesting that the process of collective problem solving can be optimized with the help of the RL.

Methods

Collective problem solving is modeled as a multi-agent search for a maximum of a given landscape, which represents a problem of a given complexity. During the search, agents can use the information shared through their social network to improve group outcomes.

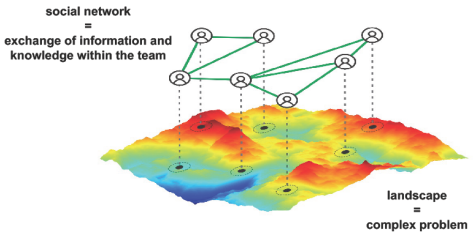

Agents explore the landscape through social learning, by consulting their nearest neighbours in the social network and copying the best (BEST) or the most frequently occurring (FREQ) fitness value. If social learning fails to identify an answer better than currently known to an agent, it tries to learn individually by exploring the landscape within proximity to its present state.

We investigate how three key factors affect the performance of teams in collaborative environments:

1. the complexity of problems facing the group, which is reflected by the roughness of the landscape

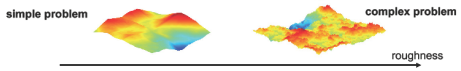

2. the structure of the network used to share the information between agents

3. the learning strategies and modes of communication between team members

Conclusion

Developed simulation environment enables us to test how the structure of a social network used to share information and the modes of information accumulation within a team affect the speed and accuracy of collective work, providing a platform for testing various C2 configurations and assessing their viability.

Key achievements include:

- Determining that the detailed structure of the social network used to share information has limited impact on the group performance and that sparsely connected teams perform equally well or better than densely connected ones.
- Showing that collective decisions are reached faster in densely connected teams, however at a cost of lower accuracy.
- Observing that intermittent switching between group work and individual work results in a significant increase in overall team performance.

Acknowledgment: This research was sponsored by the U.S. Army Research Laboratory and the U.K. Ministry of Defense under Agreement Number W911NF-16-3-0001. The views and conclusions contained in this document are those of the authors and should not be interpreted as representing the official policies, either expressed or implied, of the U.S. Army Research Laboratory, the U.S. Government, the U.K. Ministry of Defense or the U.K. Government. The U.S. and U.K. Governments are authorized to reproduce and distribute reprints for Government purposes notwithstanding any copyright notation hereon.

Rapid Evaluation of Metal-based Reactive Materials for Energetic Formulations Under High Heating Rates

Elliot R. Wainwright, Jennifer L. Gottfried
WMRD, Weapon Sciences, Detonation Science & Modeling Branch

Why Metal Reactive Materials?

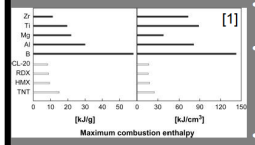

- Metals have large energy of combustion vs. high explosives
- Ability to tune microstructure/ chemistry and independently control ignition and combustion properties
- Goal: enhance and control timescale of energy release to detonation-relevant timescales

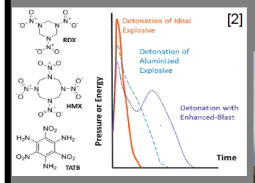

Tomahawk missile air-blast vs. target

Laser-Induced Air Shock for Energetic Materials (LASEM)

- Unique ARL-developed technique where laser-induced shock waves are used to estimate detonation performance using a few mg
- Samples material reactions from 1 µs – 100's ms

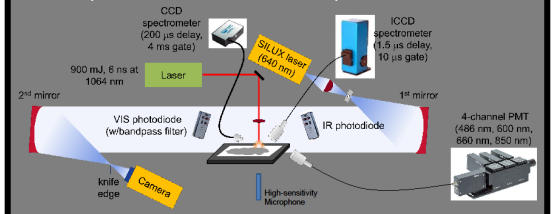

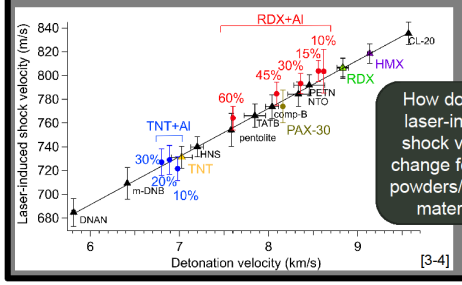

How does the laser-induced shock velocity change for metal powders/reactive materials?

[3-4]

Acoustic & Shockwave Measurements

(a) Acoustic pressure wave is measured as a time series with a far-field microphone ~ 7 cm away from the laser spot

(b) Acoustic measurements of time to peak and max amplitude of the primary shockwave correlate to optical shockwave measurements

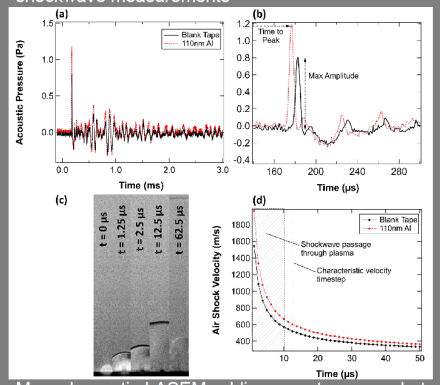

(c) Monochromatic LASEM schlieren system snapshots with formation of the plasma and shockwave propagation

(d) Velocity of the shockwave is taken via derivative of measured position vs. time, a characteristic time step of 13 µs of data fit to TNT (Dewey) blast model is used [5]

Automated Data Processing

- Higher framerate (800k fps) = easier to measure subtle differences between otherwise similar chemistry samples
- MATLAB code written with automatic edge detection
- Reduces data processing time by 10x

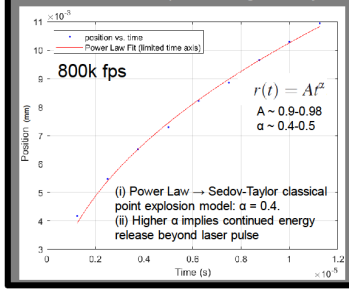

"Ashby"-style Performance Plot

- Ashby Plot: used to display performance of a class of materials under two disparate properties. Can be organized by processing parameters, chemistry, etc.
- Acoustic measurement corroborate optical shockwave measurements
- Reactive material "Ashby" plot of academic collaborator materials and common benchmarks
- Many novel reactive materials show significant enhancement of microsecond scale energy release

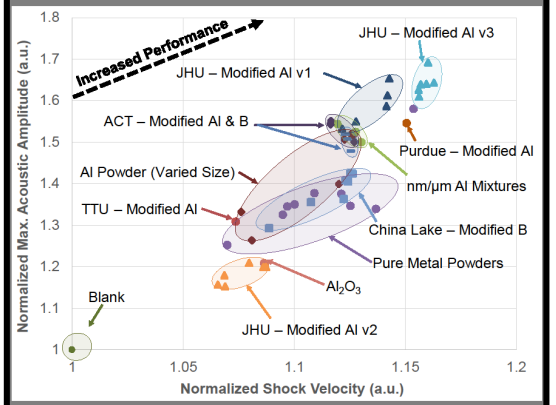

Conclusions

- Shock velocity of novel metal reactives is complex interplay of chemistry, particle size, microstructure, all affecting reactions at the 1-10 µs scale
- Understanding mechanisms of metal reactions leading to varied shock response is critical for future engineering of transformational material systems
- Can we automate the data collection for further enhanced throughput of material characterization?

References

[1] E. L. Dreizin, Prog. Eng. Combust. Sci., 35, 2, 141–167 (2009).
[2] S. M. Peiris, AIP Conference Proceedings 1979, 020002 (2018).
[3] Gottfried, PEP 40, 674 (2015).
[4] Gottfried & Bukowski, Appl. Opt. 56, B47 (2017).
[5] Dewey, John M. *Proc. Royal Soc. London. Series A. Mathematical and Physical Sciences* 279, 1378, 366-385 (1964).

XPORT ENTRAP: A DROPLET MICROFLUIDIC PLATFORM FOR ENHANCED DNA TRANSFER BETWEEN MICROBIAL SPECIES

Jose A. Wippold[1], Monica Chu[1], Bryn L. Adams[1*], Arum Han[2,3*]

(1) U.S. Army Research Laboratory DEVCOM, Biology and Biological Sciences Division, Human Research and Engineering Directorate, Biotechnology Branch, (2) Department of Electrical and Computer Engineering, Texas A&M University, (3) Department of Biomedical Engineering, Texas A&M University

High throughput introduction of DNA into cells remains a significant challenge to the widespread implementation in various microbes of synthetic biology and other genetic engineering tools. Common approaches to DNA uptake, such as competent cell transformation, electroporation, and transfection, are typically only amendable to a very small subset of laboratory bacterial strains and thus leave the vast majority of microbial life genetically inaccessible. To address this challenge, we developed a novel system named DNA ENTRAP (***DNA ENhanced TRAnsfer Platform*****),** which is a droplet-based microfluidic platform that generates nano-bioreactors, providing the capability to streamline the development of genetic transfer.

DNA ENTRAP's Technology Principles & Driving Forces

Synthetic biology is the application of the design-test-build engineering approach to the genetic structures of living, biological systems and has been described as a tool to incorporate new functions into living organisms at the DNA level (1). Droplet microfluidic technology has demonstrated utility as a screening mechanism for numerous biological applications using various types of bacteria encapsulated in droplets (2). DNA introduction into laboratory microbes, or synthetic biology chassis, such as Escherichia coli and Saccromycese cerevisiae (brewer's yeast) is a relatively easy process, utilizing common techniques such as chemically competent cells or electroporation (3). However, these methods only work for a handful of microbes, thus severely limiting potential scientific applications in which the techniques may be utilized to construct novel synthetic organisms. To this end, we present DNA ENTRAP as a system to simplify, enhance, and increase the throughput of XPORT-mediated, cell-to-cell DNA transfer events using a droplet microfluidic approach. A system that enables genetic transformation has been described, but systems that enable high-throughput, multi-parameter genetic transfer via XPORT mediated gene transfer have yet to be achieved (4-5). Despite advances in genetic engineering as a field, inducing competence into non-native cells is non-trivial and requires substantial microbiological equipment and expertise in order to successfully alter an environmental isolate in which not much information is known regarding the genome or phenotype. The system developed here, DNA ENTRAP, aims to address these limitations by circumventing the needed laboratory environments as XPORT conjugation can be conducted under harsh circumstances (6). XPORT is a novel synbio tool for DNA transfer from one microbe to another. XPORT is a specialized Bacillus subtilis strain engineered to enable an inducible control over conjugation events that integrate delivered DNA into the chromosome of a recipient cell, including unidentified environmental samples (6).

Assay Development

The platform was designed and fabricated to perform the following basic functions: generation of a large number of water-in-oil-emulsion droplets encapsulating donor and recipient cell candidates, each serving as independent nano-liter scale bioreactor; incubation of the cell-encapsulated droplets for varying times; facile ratiometric cellular encapsulation screening; and adaptability to future pairing with automation modalities.

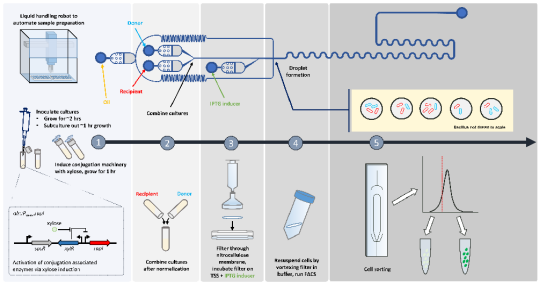

Droplet Conjugation

The underlying technology of DNA ENTRAP was tested to determine whether the system is capable of performing the relevant DNA transfer assays. Cells were co-encapsulated in droplets at two ratios 3:1 & 1:1 donor cell to recipient cell, respectively, for 0.5 hr, 1 hr, and 2 hr co-incubation periods. We determined the conjugation efficiency to be superior when using DNA ENTRAP compared to the conventional benchtop method for a 3:1 ratio at 0.5 hr, 1 hr, and 2 hr, respectively and delivering improvements on efficiency over an order of magnitude at certain timepoints.

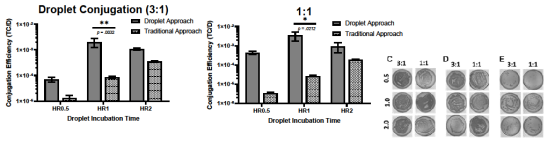

Biological Principle & Need

At the heart of DNA ENhanced TRAnsfer Platform (DNA ENTRAP), is a microfluidic device that leverages a cell-to-cell DNA transfer tool, XPORT, previously developed through a collaboration between the Massachusetts Institute of Technology and ARL (6) . This synbio tool termed XPORT utilizes a highly engineered donor Bacillus subtilis cell to transfer synthetic genetic circuits to a wide range of gram-positive recipient cells, including cells that are unidentified or uncharacterized. The XPORT technique requires the donor and recipient cells to be in physical contact with each other to facilitate DNA transfer, and often the ratio of donor to recipient cells must be quite high (10^4:1) to ensure success. While XPORT introduces a promising method for engineering undomesticated bacteria, there are limitations in that this technique is performed exclusively by hand (i.e. no robotics or automation involved) and is also very time and labor intensive, severely restricting the number of conjugations that can be attempted at one time. Thus, this system is ideal for streamlining into a high-throughput, automated microfluidic system, as the nature of XPORT mediated DNA transfer lends itself well to miniaturization into microdroplets.

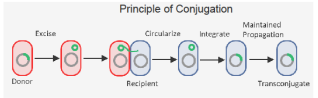

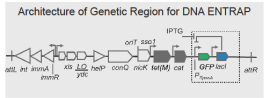

Droplet Viability

Cellular compatibility and viability were assessed using a multi-fluorescent probe strategy enabling in-droplet cell detection and viability read-out for both the B. *subtilis* JAB 981 DNA donor strain and the B. *subtilis* JAB 545 DNA recipient strain. On-chip viability experiments were conducted over a 12 hr analysis period. During this time, neither the JAB 981 or JAB 545 strains displayed any appreciable loss of viability (>99% viability).

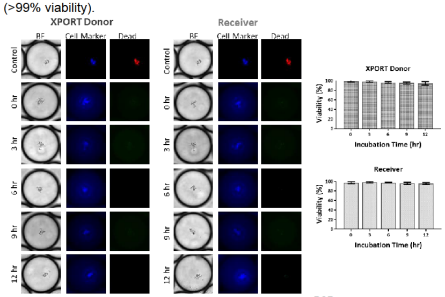

Confirmatory Assays

Following demonstration of on-chip conjugation, a confirmation analysis was performed on transconjugates to not only provide evidence that correct gene region transferred from donor to target, but also to test the performance of the transferred region. For this round of testing, a transconjugate obtained from DNA ENTRAP was obtained following a selective-media agar plate growth and then PCR amplification of the miniICE gene insert was conducted to isolate the relevant gene (see 'Sequencing confirmation' for more detail). The PCR product was then longread on a MinION to confirm the genetic makeup. DNA ENTRAP has demonstrated efficient XPORT-mediated nucleic acid transfer and thus establishes itself as the first system capable of screening the multi-parameter conditions needed to streamline the development of genetic transfer protocols.

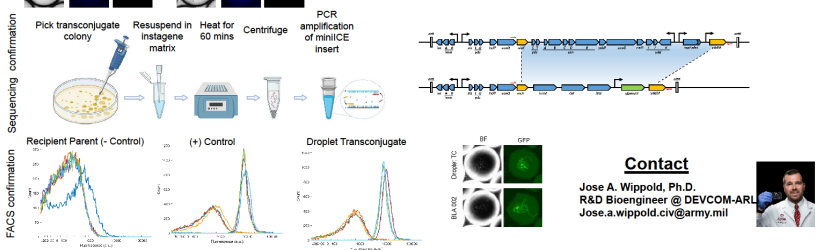

References

[1] Le Feuvre RA & Scrutton NS (2018) A living foundry for Synthetic Biological Materials: A synthetic biology roadmap to new advanced materials. Synthetic and Systems Biotechnology 3(2):105-112
[2] Kaminski TS, Scheler O, & Garstecki P (2016) Droplet microfluidics for microbiology: techniques, applications and challenges: Lab on a chip 16(12):2168-2187.
[3] Adams BL (2016) The Next Generation of Synthetic Biology Chassis: Moving Synthetic Biology from the Laboratory to the Field. ACS synthetic biology 5(12):1328-1330screening. PNAS 2009. Vol 106, no. 34: 1419501420
[4] Lam T, Maienschein-Cline M, Eddington D, & Morrison D (2020) Multiplex gene transfer by genetic transformation between isolated S. pneumoniae cells confined in microfluidic droplets. Integrative Biology 1
[5] Lam T, Brennan M, Morrison D, & Eddington D (2019) Femtoliter Droplet Confinement of Streptococcus pneumoniae: Bacterial Genetic Transformation by Cell-cell Interaction in Droplets. Lab on a chip 19.
[6] Brophy JAN, et al. (2018) Engineered integrative and conjugative elements for efficient and inducible DNA transfer to undomesticated bacteria. Nature Microbiology 3(9):1043-1053

Contact

Jose A. Wippold, Ph.D.
R&D Bioengineer @ DEVCOM-ARL
Jose.a.wippold.civ@army.mil

List of Symbols, Abbreviations, and Acronyms

6PECRD	6th Annual Postdoc and Early Career Research Day
ALC	Adelphi Laboratory Center
APG	Aberdeen Proving Ground
ARL	Army Research Laboratory
CHRO	Civilian Human Resources Office
CISD	Computational and Information Sciences Directorate
HRED	Human Research and Engineering Directorate
NPAW	National Postdoc Appreciation Week
PDA	Postdoctoral Association
Q&A	question and answer
SEDD	Sensors and Electron Devices Directorate
WMRD	Weapons and Materials Research Directorate

1 (PDF)	DEFENSE TECHNICAL INFORMATION CTR DTIC OCA
1 (PDF)	DEVCOM ARL FCDD RLB CI TECH LIB
1 (PDF)	DEVCOM ARL FCDD RLA LE L LARKIN